



Australian Government
Bureau of Meteorology

The Centre for Australian Weather and Climate Research
A partnership between CSIRO and the Bureau of Meteorology



Chemical Transport Model - Technical Description

Martin Cope, Sunhee Lee, Julie Noonan, Bill Lilley, Dale Hess and Merched Azzi

CAWCR Technical Report No. 015

October 2009



www.cawcr.gov.au



Chemical Transport Model - Technical Description

Martin Cope, Sunhee Lee, Julie Noonan, Bill Lilley, Dale Hess and Merched Azzi

CAWCR Technical Report No. 015

October 2009

ISSN: 1836-019X

ISBN: 9780643098244 (pdf.)

Series: Technical report (Centre for Australian Weather and Climate Research.) ; no.15

Enquiries should be addressed to:

Martin Cope
Centre for Australian Weather and Climate Research:
A Partnership between the Bureau of Meteorology and CSIRO

martin.cope@csiro.au

Copyright and Disclaimer

© 2009 CSIRO and the Bureau of Meteorology. To the extent permitted by law, all rights are reserved and no part of this publication covered by copyright may be reproduced or copied in any form or by any means except with the written permission of CSIRO and the Bureau of Meteorology.

CSIRO and the Bureau of Meteorology advise that the information contained in this publication comprises general statements based on scientific research. The reader is advised and needs to be aware that such information may be incomplete or unable to be used in any specific situation. No reliance or actions must therefore be made on that information without seeking prior expert professional, scientific and technical advice. To the extent permitted by law, CSIRO and the Bureau of Meteorology (including each of its employees and consultants) excludes all liability to any person for any consequences, including but not limited to all losses, damages, costs, expenses and any other compensation, arising directly or indirectly from using this publication (in part or in whole) and any information or material contained in it.

Contents

1.	OVERVIEW.....	5
2.	THE GOVERNING EQUATION.....	6
2.1	The numerical analogue	7
3.	TRANSPORT PROCESSES.....	7
3.1	Advection	8
3.2	Sub-grid scale diffusion	10
3.2.1	Horizontal diffusion	10
3.2.2	Vertical diffusion	12
3.3	Mass correction	13
3.3.1	Velocity adjustment.....	14
3.3.2	Concentration re-normalisation.....	15
4.	DEPOSITION.....	16
4.1	Dry deposition	16
4.2	Wet deposition	20
4.2.1	Uncoupled vertical transport.....	20
4.2.2	Calculation of V_{wet} - resolved clouds.....	21
4.2.3	Calculation of V_{wet} - unresolved clouds.....	22
4.2.4	Explicit vertical transport.....	23
5.	CHEMICAL TRANSFORMATION.....	23
5.1	Method of solution.....	23
5.2	The CTM chemical compiler.....	28
5.3	Chemical transformation mechanisms	35
6.	AEROSOL PROCESSES.....	36
6.1	Secondary inorganic aerosol mechanisms	36
6.2	The secondary organic aerosol mechanism.....	37
6.2.1	Method of solution	40
6.3	In-cloud sulphate production.....	45
6.3.1	Aqueous-Phase Chemical Equilibria	46
6.3.2	Method of solution	49
7.	EMISSIONS.....	52
7.1	Anthropogenic emissions.....	53
7.1.1	Motor vehicle emissions	53
7.1.2	Elevated point source	53
7.2	Natural emissions	53
7.2.1	VOC emissions from forest canopies	54
7.2.2	VOC emissions from pasture and grasses	57

7.2.3	Natural NO _x emissions	58
7.2.4	Natural NH ₃ emissions	59
7.2.5	Sea salt emissions	60
7.2.6	Wind blown dust emissions	60
7.2.7	Mercury emissions	63

REFERENCES.....	65
------------------------	-----------

APPENDIX A –CHEMICAL TRANSFORMATION MECHANISMS.....	70
--	-----------

1. NO_x mechanism.....	71
2. O_x mechanism	72
3. Generic Reaction Set Mechanism.....	73
4. Mercury mechanism.....	75
5. Lurmann, Carter, Coyner mechanism.....	76
6. Carbon Bond 2005 mechanism	84
7. Carbon Bond 2005 mechanism + aerosols	96

List of Figures

- Figure 1 Schematic diagram showing a 1-dimensional horizontal flux configuration of the vector wind components (U), the mass fluxes at the cell interfaces (F) and concentrations (C). 9
- Figure 2 Schematic diagram showing the location of the variables used to calculate horizontal diffusion. 11
- Figure 3 Schematic diagram of the resistance model used to calculate dry deposition velocity. The resistance terms are defined in the text. 18
- Figure 4 Example of the text-based input used by the chemical compiler to build a software description of a chemical transformation mechanism for use by the CTM. 29
- Figure 5 Schematic diagram showing how the predictor-corrector scheme is used to integrate eqn (6.7). 50
- Figure 6 Schematic diagram showing how a bi-section algorithm is used to solve for the charge balance shown in equation 7. 51
- Figure 7 Ambient temperature correction functions for the tailpipe emissions of NO_x (TP-NO_x), VOC (TP-VOC) and CO (TP-CO); and evaporative emissions of VOC (EVP-VOC) from petrol-driven vehicles. 54

List of Tables

Table 1 Coordinate scaling factors used by the CTM.....	6
Table 2 Description of the rate coefficient function used by the CTM chemical compiler.	30
Table 3 The photolysis rates treated by the chemical compiler.....	34
Table 4 Summary of the chemical mechanisms generated by the CTM chemical compiler.....	35
Table 5. Gas and aerosol phase species included in the MARS and ISORROPIA models.....	37
Table 6 Semi-condensable aerosol forming reactions for VOC precursor compounds	41
Table 7 Aerosol forming equilibria for SOA compounds	42
Table 8 Core and extension species used by Carbon Bond 2005 for modelling secondary organic production.	43
Table 9 Equilibrium Reactions in aqueous phase chemistry mechanism.	47
Table 10 Core and extension Carbon Bond 2005 species required by cloud chemistry and secondary aerosol models.	52
Table 11 NO _x and NH ₃ emission rates from natural landscapes.....	59
Table 12 NO _x mechanism	71
Table 13 O _x mechanism species listing	72
Table 14 O _x mechanism reactions	72
Table 15 GRS mechanism species listing.....	73
Table 16 GRS mechanism	74
Table 17 HG3T species listing.....	75
Table 18 LCC species listing.	76
Table 19. LCC mechanism.....	78
Table 20 Carbon Bond 2005 species listing.	84
Table 21 Carbon Bond 2005 reactions.....	87
Table 22 Carbon Bond + aerosol species listing	96
Table 23 Carbon Bond 2005 + aerosol mechanism	100

1. OVERVIEW

In the following pages we provide a technical summary of the CSIRO chemical-transport modelling system (the CTM). The system comprises an Eulerian modelling framework which is designed to model the emission, transport, chemical transformation and deposition of a gas phase- or a mixed gas and aerosol phase system. The CTM is typically used for modelling urban- and regional scale photochemical smog production, including primary and secondary aerosol mass.

The CTM is coupled to the Carbon Bond 2005 mechanism, (Yarwood et al 2005); the Lurmann, Carter, Coyner mechanism (Lurmann et al. 1987); and the Generic Reaction Set mechanism (Azzi et al. 1992) for modelling photochemical smog transformation. With respect to reactive aerosols, the CTM includes a module for simulating the thermodynamic steady-state concentrations of an aerosol sulfate, nitrate, ammonium, water system (Saxena et al. 1986); and modules for simulating secondary organic aerosol production and sulfate production within cloud water.

The CTM has inline algorithms for calculating the natural emissions of volatile organic compounds (VOCs) from vegetation and the emissions of oxides of nitrogen (NO_x) and ammonia from soils. The CTM also includes algorithms for calculating the emission of gaseous elemental mercury from vegetation, soils and water; and the emission of sea salt aerosol and wind blown dust.

The CTM is currently run operationally by the Bureau of Meteorology as part of the Australian Air Quality Forecasting System (Cope et al. 2004) and has been coupled offline to the Bureau of Meteorology Limited Area Prediction System (LAPS) for this purpose (Puri et al. 1998). The CTM has also been coupled offline to the CSIRO Conformal Cubic Model (CCAM; McGregor 2005) for the simulation of mercury transport and deposition across the Australian continent, and additionally has been coupled inline with TAPM (Hurley 2008). This version (known as TAPM-CTM) has been used extensively for modelling urban-scale photochemical smog under current-day and potential climate change conditions (Cope et al. 2009).

2. THE GOVERNING EQUATION

The governing equation for the CTM is the semi-empirical advection-diffusion equation for reactive species, here written for a single species, and in a scaled flux form (Toon et al. 1988), in which geometric scaling factors are introduced into the governing equation to enable the CTM to be coupled to meteorological models which are formulated in a variety of coordinate systems.

$$\frac{\partial C^*}{\partial t} + \frac{\partial UC^*}{\partial X} + \frac{\partial VC^*}{\partial Y} + \frac{\partial WC^*}{\partial \sigma} =$$

$$\frac{\partial}{\partial X} \rho^* K_1 \frac{\partial C^*/\rho^*}{\partial X} + \frac{\partial}{\partial Y} \rho^* K_2 \frac{\partial C^*/\rho^*}{\partial Y} + \frac{\partial}{\partial \sigma} \rho^* K_3 \frac{\partial C^*/\rho^*}{\partial \sigma} + (P-L)V_m M_1 M_2$$
(2.1)

Here C^* is the scaled concentration ($C^* = C/V_m M_1 M_2$ where the unscaled concentration C is expressed as a mass density i.e. g m^{-3} or molec cm^{-3}), ρ^* is the scaled atmospheric density ($\rho^* = \rho_a/V_m M_1 M_2$), U , V and W are scaled velocities ($U=u/M_1$, $V=v/M_2$, $W=w/V_m$) in the X , Y and σ directions (and u , v , w are the corresponding Cartesian velocity components), $K_{1,2}$ are the scaled horizontal components of the eddy diffusivities, and K_h is the scaled vertical eddy diffusivity ($K_1=K_h/M_1^2$, $K_2=K_h/M_2^2$, $K_3=K_z/V_m^2$), P is the rate of change due to chemical production and emission, and L is loss rate through chemical transformation and wet- and dry deposition. The horizontal and vertical scale factors M_1 , M_2 , and V_m are chosen to match those used by the host meteorological model (Table 1).

Table 1 Coordinate scaling factors used by the CTM.

Host Model	Horizontal coordinate system	Scaling Factors			Vertical coordinate system	Scaling Factor
		M_1	M_2	M_3		
		M_1	M_2	M_3		$V_m = \partial z / \partial \sigma$
LAPS	Spherical	$\cos(\theta)$	1.0	R_e	p/p_s	$p_s/\rho_a g$
CCAM	Spherical	$\cos(\theta)$	1.0	R_e	p/p_s	$p_s/\rho_a g$
TAPM	Rectangular	1.0	1.0	1.0	$(z - z_s)/(z_t - z_s) \times z_t$	$z_t/(z_t - z_s)$

R_e =earth radius; p =pressure; p_s =surface pressure; z = height above sea level; z_s = ground height; z_t = top of model domain; g = gravity; ρ_a = air density

2.1 The numerical analogue

The solution of eqn (2.1) is achieved by splitting the multi-dimensional problem into a set of one-dimensional solutions using to the method of Marchuk (1974). This enables optimal numerical solution algorithms to be selected for each modelled process.

A single time-level, quasi-second order accurate (in time) solution to eqn (2.1) is given by

$$C^*(t + 2\Delta t) = T_x T_Y T_\sigma M_c D_h [V_w (D_v E_s C_g) C_{aq} P_{sio} P_{soa} 2\Delta t] D_h T_\sigma T_Y T_x M_c C^*(t) \quad (2.2)$$

where T_i (eg. T_x) represents the advection operator in the i^{th} coordinate direction, M_c is a mass correction step, D_h is the horizontal diffusion operator, D_v is the vertical diffusion operator, V_w is the wet deposition operator, E_s is an emission term, and C_g is the gas phase chemical transformation operator C_{aq} is the aqueous phase operator, P_{sio} is the secondary inorganic aerosol operator and P_{soa} is the secondary organic aerosol operator. One cycle of eqn (2.2) integrates the CTM for a period $2\Delta t$ (s).

Provided the total integration time step is not too large, the error introduced by operator splitting can be kept within a few percent. Typically the following time step limitation is used for the operator splitting.

$$\Delta t = \begin{cases} 150 & \Delta t_{Txy} \geq 150 \\ \Delta t_{Txy} & \Delta t_{Txy} < 150 \end{cases} \quad (2.3)$$

Here a time step of 150s corresponds to half the TAPM integration time step [thus (2.2) integrates the CTM for a single TAPM time step), and Δt_{Txy} corresponds to a time step such that the maximum Courant number ($C = u\Delta t/\Delta x$) of the horizontal advection operator is less than one.

3. TRANSPORT PROCESSES

The CTM transport processes consist of horizontal and vertical advection, horizontal and vertical sub-grid scale turbulent diffusion, and the transport sinks of dry and wet deposition. The advection and turbulent diffusion transport processes are modelled with one-dimensional versions of the relevant equations as discussed in sections 3.1 and 3.2. Dry deposition is treated as a lower boundary condition to the vertical diffusion process (section 4.1). The transport of mass in rain (and the subsequent wet deposition at the surface) is either treated as an explicit

advection process and hence is solved by the T_σ operator; or is treated as an instantaneous transport process (section 4.2). At the current time the choice of wet deposition transport methodology depends upon whether the CTM is run inline in TAPM (and hence has access to more detailed cloud droplet information); and whether a detailed in-cloud sulphate chemistry is selected. This is discussed further in section 4.2.

3.1 Advection

The processes of horizontal and vertical advection are represented by the following set of partial differential equations.

$$\frac{\partial C^*}{\partial t} + \frac{\partial UC^*}{\partial X} = 0 \quad (3.1a)$$

$$\frac{\partial C^*}{\partial t} + \frac{\partial VC^*}{\partial Y} = 0 \quad (3.1b)$$

$$\frac{\partial C^*}{\partial t} + \frac{\partial WC^*}{\partial \sigma} = 0 \quad (3.1c)$$

Eqn (3.1) is solved with the Blackman constrained cubic scheme of Yamartino (1993), a high-order, flux-based scheme that uses spectral conditioning, sub-grid linear interpolation, donor-cell allocation and supplementary non-linear filtering to achieve a positive-definite solution under conditions of strong concentration gradient. This scheme has been specifically developed for use in Eulerian air quality modelling systems and exhibits excellent retention of peak and shape for short wavelength signals.

The concentration at time level n is advanced to time level $n+1$ as follows (here for east-west transport).

$$C_{ij}^{n+1} = C_{in}^n - (F_{i+1/2} - F_{i-1/2}) \frac{\Delta t}{\Delta x} \quad (3.2)$$

Here C_{ij} is the concentration in cell ij as shown in Figure 1, and Δx is the horizontal cell spacing and the cells are assumed to be of constant height. The flux through the cell interface $i-1/2$ is given by

$$F_{i-1/2} = U_{i-1/2} \langle C \rangle \quad (3.3)$$

where $\langle C \rangle$ is the Crowley integral of the concentration from $x_{i-1/2}$ to a distance $U_{i-1/2}\Delta t$ upwind of the cell face. The concentration within the integral is initially prescribed by a cubic interpolation function which is fitted to the concentrations C_{ij} and then treated by various methods to ensure positivity of $C_{i,j}$. Thus

$$C(x) = a_0 + a_1s + a_2s^2 + a_3s^3 \tag{3.4a}$$

where the domain of s is $-1/2 \leq s \leq 1/2$ and a_i are selected to provide optimal accuracy to the piecewise cubic and the cubic coefficients are defined as follows.

$$\begin{aligned} a_0 &= C_{i,j} \\ a_1 &= D_{i,j}\Delta x \\ a_2 &= \frac{1}{4}(C_{i+1,j} - 2C_{i,j} + C_{i-1,j}) + \frac{3\Delta x}{8}(D_{i+1,j} - D_{i-1,j}) \\ a_3 &= C_{i+1,j} - C_{i-1,j} - \frac{\Delta x}{6}(D_{i+1,j} + 10D_{i,j} + D_{i-1,j}) \end{aligned} \tag{3.4b}$$

and $D_{i,j}$ are the derivatives.

One of the methods used to ensure positivity of $C_{i,j}$ is the spectral limiting of the coefficients.

$$\left| \frac{a_j}{a_0} \right| < \frac{\pi^j}{j!} \tag{3.5}$$

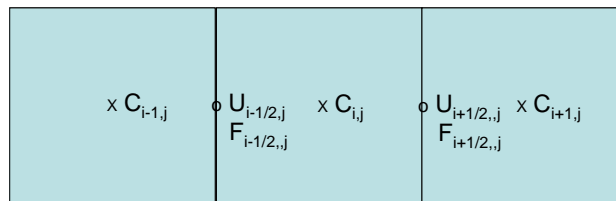


Figure 1 Schematic diagram showing a 1-dimensional horizontal flux configuration of the vector wind components (U), the mass fluxes at the cell interfaces (F) and concentrations (C).

Positivity is also ensured by approximating eqn (3.4a) by multiple straight-line, sub-grid segments which are constrained to be greater than zero.

Boundary conditions are given as follows.

$$uc = uc_{in} \quad \text{inflow} \quad (3.6a)$$

$$\partial F / \partial x = 0 \quad \text{outflow} \quad (3.6b)$$

where c_{in} is a prescribed boundary concentration and eqn (3.6b) corresponds to a zero flux divergence outflow (EPA 1999). Following the solution of eqn (3.2), a minimally diffusive filter is applied to remove short wavelength minima or maxima which may have been generated by the advection process (see Yamartino 1993 for more details).

3.2 Sub-grid scale diffusion

The process of sub-grid scale transport is modelled using the first order closure approximation with the eddy diffusivities either derived internally by the CTM using standard meteorological variables (such as the wind, temperature and surface variables), or interpolated from the eddy diffusivity fields generated by the host meteorological model (currently restricted to TAPM-CTM).

3.2.1 Horizontal diffusion

Horizontal diffusion is modelled using eqn (3.7) and represents gradient transport as a process which is driven by the mixing ratio gradient rather than the gradient in mass density, and thus the concentration is first normalised by the atmospheric density.

$$\begin{aligned} \frac{\partial C^*}{\partial t} - \frac{\partial}{\partial X} \rho^* K_1 \frac{\partial C^* / \rho^*}{\partial X} &= 0 \\ \frac{\partial C^*}{\partial t} - \frac{\partial}{\partial Y} \rho^* K_2 \frac{\partial C^* / \rho^*}{\partial Y} &= 0 \end{aligned} \quad (3.7)$$

As discussed above, the eddy diffusivities are either taken directly from the meteorological model, or alternatively are derived from standard meteorological fields. For the latter case, two processes of horizontal diffusion are considered, with the first process being plume growth due to distortion or stress in the horizontal transport field. This is modelled using the approach of Smagorinsky (1963) where (for the unscaled horizontal eddy diffusivity).

$$K_h = \left[(dv/dx + du/dy)^2 + (du/dx - dv/dy)^2 \right]^{1/2} \quad (3.8)$$

Sub-grid-scale turbulence is the second process to be considered and is parameterised as follows (Hess 1989).

$$K_h = \begin{cases} 0.143u_*h(z/h)(1-z/h)^{1/2} & z < h; L \geq 0 \\ 0.1w_*h & z < h; L < 0 \\ 0.001 & z \geq h \end{cases} \quad \begin{matrix} (3.9a) \\ (3.9b) \\ (3.9c) \end{matrix}$$

where u_* is the friction velocity, h the boundary layer height, w_* the convective velocity scale and L is the Obukhov length.

The two components of K_h are then combined to yield a total horizontal diffusion rate, which is scaled by the appropriate geometric map factors (Table 1) before being applied in eqn (3.7).

The horizontal diffusion equations are solved using a 2nd order in space explicit differencing scheme which uses the concentration, density and eddy diffusivities are located as shown in Figure 2.

$$C_i^{n+1} = C_i^n \left[1 - \frac{\Delta t}{\Delta x^2} \left(\frac{\rho_{i+1/2}}{\rho_i} K_{i+1/2} + \frac{\rho_{i-1/2}}{\rho_i} K_{i-1/2} \right) \right] + \frac{\Delta t}{\Delta x^2} \left(\frac{\rho_{i+1/2}}{\rho_{i+1}} K_{i+1/2} C_{i+1} + \frac{\rho_{i-1/2}}{\rho_{i-1}} K_{i-1/2} C_{i-1} \right) \quad (3.10)$$

(note that the subscript 'a' has been omitted from the atmospheric density in eqn (3.10) for brevity).

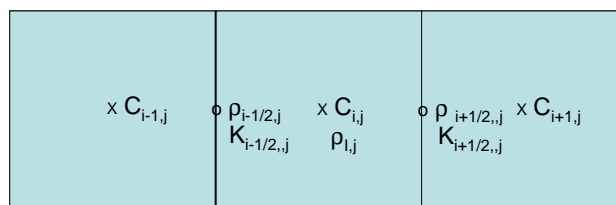


Figure 2 Schematic diagram showing the location of the variables used to calculate horizontal diffusion.

Because eqn (3.10) is an explicit scheme, it is necessary to limit the time step so that the Courant number $(dt/dx^2 K_h) < 0.5$. This is done by solving the diffusion equation for a series of sub-time steps until the full integration time step Δt is reached.

3.2.2 Vertical diffusion

The vertical diffusion is solved during the chemical transformation step together with the concentration tendencies due to emissions and dry deposition (see eqn 2.2). This is done because these processes are strongly coupled in surface layer, particularly in an urban area where the majority of the sources are located close to ground level. Because chemical transformation is solved in an unscaled form in Cartesian coordinate space, the vertical diffusion equation is also written in Cartesian form.

$$\frac{\partial C}{\partial t} - \frac{\partial}{\partial z} \rho_a K_z \frac{\partial C}{\partial z} = 0 \quad (3.11)$$

The vertical diffusion coefficients are calculated using the Hysplit scheme (Draxler and Hess 1997). Within the surface layer ($z/h < 0.1$), the vertical diffusivity is given by

$$K_z = [ku_*/\phi_h(z/L)] z(1 - z/h)^2 \quad (3.12)$$

Where k is von Karman's constant (0.40) and ϕ_h is the normalised profile for heat.

$$\phi_h = \begin{cases} 0.64 \left[(3.0 - 2.5 * z/L) / (1.0 - 10z/L + 50(z/L)^2) \right]^{1/3} & z/L < 0 \\ \text{Pr}_n \left\{ 1.0 + z/L \left[(1.0 + 2/3z/L)^{0.5} + \right. \right. \\ \left. \left. 2/3 \exp(-0.35z/L)(1.0 - 0.35z/L + 5.0) \right] \right\} & z/L \geq 0 \end{cases} \quad (3.13)$$

and Pr_n is the Prandtl number for neutral conditions (0.923).

For cells located above the surface layer but within the boundary layer ($0.1 \leq z/h < 1.0$) the vertical diffusivity is given by

$$K_z = (kw_m/\text{Pr}) z(1 - z/h)^2 \quad (3.14)$$

where the velocity scale w_m is given by a weighted average of the friction velocity and w_* is the convective velocity scale.

$$w_m = (u_*^3 + 0.6w_*^3)^{1/3} \quad (3.15)$$

and the diabatic Prandtl number is given by

$$\text{Pr} = \phi_h(z_s/L) / \phi_m(z_s/L) + 7.2k(z/h)(w_*/w_m) \quad (3.16)$$

Here $z_s = 0.1h$ is the height of the surface layer and ϕ_m is the normalised profile for momentum.

$$\phi_m = \begin{cases} 1 + z/L[1 + 2/3 \exp(-0.35z/L)(1 - 0.35z/L + 5)] & z/L < 0. \\ \{[1 + 0.625(z/L)^2] / (1 - 7.5z/L)\}^{1/3} & z/L \geq 0. \end{cases} \quad (3.17)$$

Above the boundary layer the vertical diffusion coefficient is parameterised as a function of the local Obukhov length (L_0) and a Blackadar-type mixing length ($\ell = kz^{-1} + 150^{-1}$).

$$K_z = \ell^2 [(\partial u / \partial z)^2 + (\partial v / \partial z)^2]^{1/2} / [\phi_h(\ell / L_0)] \quad (3.18)$$

$$z/L = \begin{cases} 1.0893 Ri_b & Ri_b < 0.001 \\ -1.0063 \times 10^{-3} Ri_b^4 + 0.509 \times 10^{-2} Ri_b^3 + 1.6583 Ri_b^2 + 0.8049 Ri_b + 0.0.2828 \times 10^{-3} & Ri_b \geq 0.001 \end{cases}$$

$$\text{and } Ri_b = g/T \frac{(\partial \theta / \partial z)}{[(\partial u / \partial z)^2 + (\partial v / \partial z)^2]^{1/2}}$$

The vertical diffusion equation is discretised into a second-order accurate, explicit form, which is then re-arranged into the form of a first order chemical reaction scheme (by defining product and loss terms) as discussed in section 5.1. Vertical diffusion rates are then added to the formation and loss terms generated by the photochemical transformation scheme and solved by the photochemical integration scheme.

3.3 Mass correction

Being expressed in the flux form, the advection components of eqn (2.1) conserve mass provided the 3-D vector wind field is mass consistent. However, mass consistency is not guaranteed for numerical weather prediction systems when they are based on the primitive form of the governing equations. Moreover, mass errors are also introduced through the process of spatially and temporally interpolating the transport fields to the CTM grid. Additionally, the use of operating splitting to solve the 3-D advection as a series of one-dimensional advection problems [eqn (3.1)] introduces truncation errors which scale with the magnitude of the

solution time step. Kitada (1987) demonstrated that mass conservation errors are equivalent to a chemical transformation source term and thus can propagate through the species concentration fields via the coupled non-linear chemistry. Given these potential issues, it is important to undertake a mass correction step prior to undertaking the chemical transformation step.

In the CTM, we use a combination of a velocity adjustment methodology [which is similar to that of Odman and Russell (2000)] and the concentration renormalisation methodology of Byun (1999) to correct mass errors in the advection step.

3.3.1 Velocity adjustment

Following Odman and Russell (2000) the mass conservation equation eqn (3.19) is used to generate a mass consistent three-dimensional wind field through adjustments to the vertical velocity field.

$$\frac{\partial \rho^*}{\partial t} + \frac{\partial U \rho^*}{\partial X} + \frac{\partial V \rho^*}{\partial Y} + \frac{\partial W \rho^*}{\partial \sigma} = 0 \quad (3.19)$$

However in contrast to Odman and Russell who adjust the vertical velocity following a horizontal advection step, we apply eqn (3.19) prior to the advection stage with the intent of providing (to first order) a mass consistent wind field following interpolation (in space and possibly in time) of the meteorological model fields to the CTM grid.

Thus if U, V, ρ^* are the scaled horizontal vector wind field and scalar density field on the CTM grid (interpolated from the meteorological model) a first-order accurate mass consistent wind field can be generated by using eqn (3.20) to derive the vertical velocity field (W).

$$W_{i,j}^{k+1/2} = \frac{1}{\rho^{*k+1/2}} \left\{ \left(\rho^* W_{i,j} \right)^{k-1/2} - \Delta \sigma \left[\frac{(U \rho^*)_{i+1/2,j}^k - (U \rho^*)_{i-1/2,j}^k}{\Delta X} + \frac{(V \rho^*)_{i,j+1/2}^k - (V \rho^*)_{i,j-1/2}^k}{\Delta Y} + \frac{\rho_k^{*n+1} - \rho_k^{*n}}{\Delta t} \right] \right\} \quad (3.20)$$

with the non-slip lower boundary condition $W_{i,j}^{-1/2} = 0$.

In eqn (3.20), the vertical velocity has been derived for cell i,j,k . Locations $i-1/2$; $i+1/2$ refer to the faces of cell i,j in the east-west direction as shown in Figure 1. Locations $k-1/2$ and $k+1/2$ refer to

the bottom and top face of the cell and ρ_k^{*n+1}, ρ_k^n refer to the cell density at location k (the horizontal indices have been omitted for brevity) at time level n and $n+1$ and are taken from the meteorological model. Equation (3.20) yields a vertical velocity which has been constrained by the local mass conservation. The equation is solved from the surface to the top of the model domain and accumulates any mass conservation errors up through a vertical model column. The field of W derived by this approach is then used in equation (3.1) to calculate the vertical advection of each gaseous and aerosol species.

3.3.2 Concentration re-normalisation

Although the approach described above will generate a mass consistent wind field, truncation errors resulting from use of operator splitting and a high order, non linear 1-D advection scheme (section 3.1) will still lead to mass conservation errors. In order to minimise this error CTM uses the renormalisation approach of Byun (1999) to correct the concentration fields prior to the chemical transformation step. This approach is based on density scaling and compares the density at time level $n+1$ derived by solving eqn (3.19) with the T_σ operator with the density at time level $n+1$ as derived from the meteorological model output fields. Any differences between these densities are assumed to result from operator splitting errors and to be the cause of mass conservation errors. If it is further assumed that the concentration field of each species is subjected to the same error then the concentration fields can be corrected for mass conservation errors using the ratio of the advected density and the meteorological model density.

$$C_c^{n+1} = C^{n+1} \frac{\rho_{nwp}^{*n+1}}{\rho_{ctm}^{*n+1}} \quad (3.21)$$

Here C_c^{n+1} is the corrected concentration at time level $n+1$ (spatial indices have been omitted for brevity), C^{n+1} is the uncorrected concentration, ρ_{nwp}^{*n+1} is the meteorological model prediction of the density and ρ_{ctm}^{*n+1} is the density predicted after the advection step.

Note that the methodologies described above still represent a compromise solution to the mass consistency issue. Hu and Odman (2008) have shown that the density scaling methodology can cause the global mass conservation to be violated, with mass steadily increasing over an integration period. This problem can be avoided by using the velocity adjustment method of

Odman and Russell (2000); however use of the latter in isolation can lead to vertical transport errors because W accumulates mass conservation errors, potentially leading to significant transport errors for air parcel trajectories in regions of strong horizontal wind shear and enhanced vertical velocities (such as occur in regions of elevated terrain).

4. DEPOSITION

The CTM simulates the transport and loss of species mass at the earth's surface through the processes of dry and wet deposition. Dry deposition refers to the uptake of mass at the earth's surface through the processes of turbulent and molecular transport (and sedimentation for particles) and assimilation (and loss) of the mass into the stomata of leaves, the surfaces of soil particles and into water bodies. This is discussed further in the next section. Wet deposition refers to the transport of soluble species mass to the earth's surface within rain drops and is discussed in section 4.2 and section 6.3.

4.1 Dry deposition

Dry deposition is modelled as a boundary condition to the vertical diffusion process and thus is treated by the vertical diffusion operator. When expressed in a Cartesian coordinate system (and ignoring vertical gradients in the density), the equation for vertical diffusion is given as follows.

$$\frac{\partial C}{\partial t} = \frac{\partial}{\partial z} K_z \frac{\partial C}{\partial z} \quad (4.1)$$

Defining the vertical mass flux at the surface as $K_z \partial C / \partial z = -V_{dry} C$ and taking a finite difference representation of the second spatial derivative gives the following.

$$\frac{\partial C}{\partial t} = -\frac{V_{dry} C}{\Delta Z} \quad (4.2)$$

where V_{dry} is the dry deposition velocity and ΔZ is the thickness of the first model layer.

Following Wesely (1989) and EPA (1999), the dry deposition velocity is modelled using the resistance analogue approach. This is demonstrated in Figure 3 for a mixed water, vegetation, soil and urban system. The basis of the approach is that the mass flux from the atmosphere to a

sink at the surface is driven by the concentration difference between the atmosphere and the sink (which equals the atmospheric concentration C for an irreversible process) divided by a bulk resistance which is the inverse of the dry deposition velocity (hence V_{dry} which has units of $m\ s^{-1}$ is equivalent to an electrical conductance).

The CTM treats each grid cell as being entirely water or land based. Considering a water surface,

$$V_{dry} = (r_a + r_l + r_w)^{-1} \quad (4.3)$$

r_a is the aerodynamic resistance; $r_a = 1/ku_* \{ \ln(z_r/z_0) - [\psi_h(z_r/L) - \psi_h(z_0/L)] \}$

where z_r is the reference height of the concentration (here half the height of the first model layer) and z_0 is the momentum roughness. The function ψ_h is the stability correction for heat and is calculated from ϕ_h (Draxler and Hess 1997).

The laminar sub-layer resistances is given by

$$r_l = 1/ku_* \ln(z_0/z_h) \quad (4.4)$$

where z_h is the surface roughness for heat transfer.

The uptake resistance for the transfer of a gas into the aqueous phase is given by

$$r_w = c_w HRTf_0/u_* \quad (4.5)$$

where $c_w = 4.8 \times 10^{-4}$, H is the Henry's law constant ($M\ atm^{-1}$), R is the ideal gas constant ($R=0.08205\ M\ atm^{-1}\ K^{-1}$), T is the ambient temperature (K) and f_0 is an enhancement factor for H (thereby giving an effective Henry's law constant) which parameterises the loss of $C(aq)$ through aqueous phase reactions.

The urban uptake resistance r_u is currently set to the soil resistance r_{sl} where, following Wesely (1989),

$$r_{sl} = \left[\frac{f_0}{r_{gs} O} + \frac{H}{10^5 r_{gs} S} \right]^{-1} \quad (4.6)$$

DEPOSITION

with the surface resistances for oxidant and sulphur compounds given as

$$r_{gs}O, r_{gs}S = 400s \cdot m^{-1}$$

Within the vegetation canopy we define r_{st} as the canopy scale stomatal resistance (which is defined by the meteorological model) and r_m is the mesophyll resistance which is defined as follows.

$$r_m = \left(\frac{H}{3000} + 100f_0 \right)^{-1} \quad (4.7)$$

and r_{cd} , and r_{cw} are the cuticle resistances for the dry and wet part of the leaf surface ,

$$r_{cd,w} = r_{lu} (10^{-5} H + f_0)^{-1} \quad (4.8)$$

where $r_{lu} = 4000 s m^{-1}$ (dry) and $2.4 \times 10^8 s m^{-1}$ (wet).

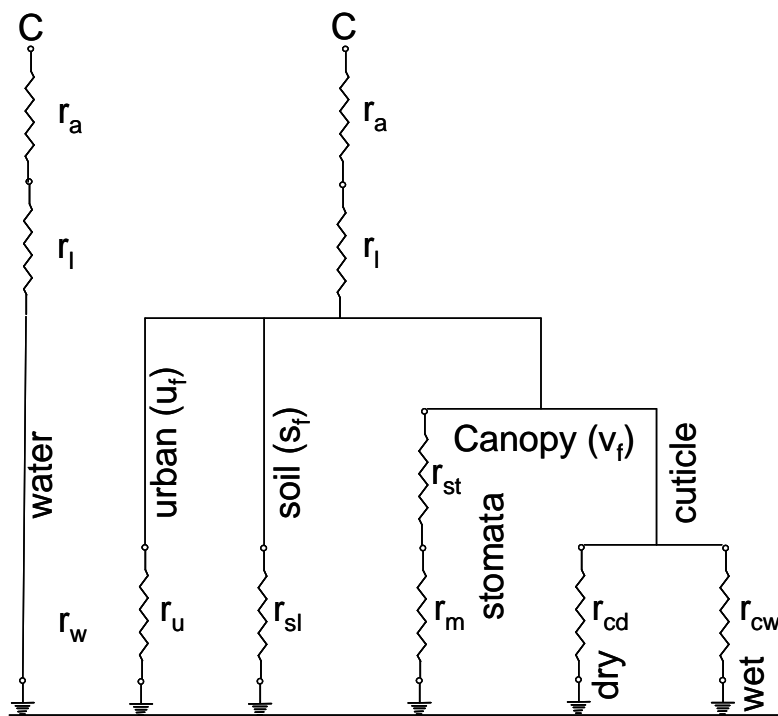


Figure 3 Schematic diagram of the resistance model used to calculate dry deposition velocity. The resistance terms are defined in the text.

Combining the in-canopy resistances gives the total canopy resistance r_c ($s m^{-1}$) as follows.

$$r_c = \frac{1}{lai} \left\{ \frac{1}{r_{st} Sc + r_m} + \left[\frac{(1-w_f)}{r_{cd}} + \frac{(w_f)}{r_{cw}} + \right] \right\}^{-1} \quad (4.9)$$

where lai is the canopy leaf area index (m^2 leaf coverage per m^2 ground area), r_{st} is the leaf level stomatal resistance ($s\ m^{-1}$) which is supplied by the meteorological model; Sc is the Schmidt number $Sc = mw_s / mw_{H20}$ where mw_s , mw_{H20} are the molecular weights of the trace gas species and water respectively, w_f is the wetted fraction of the leaves.

The dry deposition velocity is then calculated as follows.

$$v_{dry} = \frac{u_f}{r_a + r_l + r_u} + \frac{s_f}{r_a + r_l + r_{sl}} + \frac{v_f}{r_a + r_l + r_c} \quad (4.10)$$

where u_f is the urban fraction, s_f is the soil fraction and v_f is the vegetation fraction.

In the CTM, eqn (4.2) is first solved analytically to diagnose the dry deposition mass for storage into an output file. If the concentration change due to depositional loss over the course of a model time step is given as follows,

$$C(t + \Delta t) = C(t) \exp\left(\frac{-V_{dry}}{\Delta z} \Delta t\right) \quad (4.11)$$

then it follows that the mass lost to dry deposition is given by

$$\begin{aligned} M_{dry} &= [C(t + \Delta t) - C(t)] \Delta z \\ &= C(t) \left[1 - \exp\left(\frac{-V_{dry}}{\Delta z} \Delta t\right) \right] \Delta z \end{aligned} \quad (4.12)$$

Following the diagnosis of the deposition mass, the deposition tendency terms are incorporated into the vertical diffusion equation as a surface boundary condition and solved as part of the coupled chemical transformation, emission, vertical diffusion system (see section 5.1).

4.2 Wet deposition

The CTM contains two wet deposition algorithms. When the CTM is run offline, and/or wet deposition is calculated for species other than the S(VI) system described in section 6.3, then wet deposition is calculated from the rainfall rate at the surface and the vertical transport between the precipitating cloud and the surface is assumed to be instantaneous. This approach is described in the next section. If the CTM is run inline in the host meteorological model (currently only an option for TAPM-CTM) and the option to model aqueous phase S(VI) production is selected then the vertical transport and wet deposition of S(VI) and other dissolved species is modelled explicitly using the vertical advection equation [eqn (3.1)] with W augmented by the terminal velocity of the rain drops. This approach is discussed in section 4.2.1.

4.2.1 Uncoupled vertical transport

For cases in which detailed cloud microphysical data are not available from the host meteorological model, the CTM uses a wet deposition algorithm which is based on the schemes used in Hysplit (Draxler and Hess 1997) and CMAQ (EPA 1999), with additional background theory as given in Seinfeld and Pandis (1998).

The underlying premise is that the wet deposition can be described as follows-

$$\frac{\partial C}{\partial t} = -\frac{V_{wet} C}{\Delta Z} \quad (4.13)$$

Where C is the gaseous or aerosol mass concentration (kg m^{-3}) and ΔZ (m) is the depth of the layer from which the pollutant mass is being scavenged.

Note that V_{wet} is a function of the precipitation rate and the partitioning of the in-cloud pollutant mass concentration between the cloud-air and the cloud-water.

If we define a reciprocal time constant (s^{-1}) for the wet deposition as follows

$$\beta_{wet} = \frac{V_{wet}}{\Delta Z} \quad (4.14)$$

then eqn (4.13) can be integrated to give the concentration change occurring over a time interval Δt (s) (which will typically be the advection time step of the model).

$$\Delta C^k = C^k (\exp[-\beta_{wet}^k \Delta t] - 1) \quad (4.15)$$

Here the concentration change (kg m^{-3}) due to wet deposition has been calculated for level k in the precipitating cloud column.

The wet deposition (kg m^{-2}) due to precipitation from layer k in a cloud for the time period Δt is given by.

$$D^k = C^k \{1 - \exp[-\beta^k \Delta t]\} \Delta Z^k \quad (4.16)$$

The total wet deposition for the column is then given by

$$D^{total} = \sum_{kstart}^{kend} D^k \quad (4.17)$$

Where $kstart$ is the first level within the precipitating cloud and $kend$ is the final level within the precipitating cloud.

4.2.2 Calculation of V_{wet} - resolved clouds

Resolved clouds consist of large scale clouds such as stratus, cumulus or cirrus which cover entire grid cells of the model and which may persist for multiple model time steps. A resolved cloud is described by the grid cell cloud water content which is provided either as a cloud liquid water density L_c (kg m^{-3}), or as a mixing ratio q_c (kg kg^{-1}) as described in section 4.2.4 and $L_c = q_c \rho_a$.

For resolved clouds, the vertical variation in L_c may be used to partition the surface precipitation rate P_r (m s^{-1}) between the layers of the precipitation cloud according to the approach used in CMAQ (EPA 1999),

$$P_r^k = P_r \frac{L_c^k}{\sum L_c^k} \quad (4.18)$$

where the summation is taken over all column levels in which cloud is present.

The wet deposition rate for an individual species V_{wet} may then be calculated as follows

Gas

$$V_{wet} = \frac{HRT}{1 + HRTL_c / \rho_w} P_r \quad (4.19)$$

Where, as previously described, H is the Henry's constant for the gas under consideration ($\text{mol L}^{-1} \text{atm}^{-1}$), T is the ambient temperature (K), R is the universal gas constant ($0.08205 \text{ atm L mol}^{-1} \text{K}^{-1}$) and ρ_w (kg m^{-3}) is the density of water and P_r is the precipitation rate (m s^{-1}).

Aerosol

If we define a scavenging ratio E [$0-1 \times 10^6$] for an aerosol in cloud-water then eqn (4.19) may be modified as follows for an aerosol.

$$V_{wet} = \frac{E}{1 + EL_c / \rho_w} P_r \quad (4.20)$$

4.2.3 Calculation of V_{wet} - unresolved clouds

The modelled convective rainfall (sub-grid scale cloud) typically does not have the accompanying fields of cloud water from which V_{wet} may be calculated as defined above.

Generally the only available information is the convective rainfall total at the surface and the height of the base and top of the convective cloud. As a result the CTM approach for modelling wet deposition from convective clouds is very simple.

If we assume that the typical lifetime of a convective cloud is one hour ($\tau_{cloud} = 3600s$) and define the modelled convective cloud thickness as ΔZ_c in the vertical, then the average liquid water content of the cloud is given as follows.

$$L_c = \frac{\tau_{cloud} \rho_w P_r}{\Delta Z_c} \quad (4.21)$$

Once L_c has been determined, the wet deposition velocity can be calculated according to the methodology used for the resolved clouds.

4.2.4 Explicit vertical transport

The explicit vertical transport approach is that same as that used in TAPM (Hurley 2008) where it is assumed that the vertical mass flux of a dissolved species is given by the terminal velocity of the raindrops. Thus

$$V_{TR} = -\frac{a_R \Gamma(4.5)}{6\lambda_R^{0.5}} \left(\frac{\rho_w}{\rho_a} \right)^{1/2} \quad (4.22)$$

where V_{TR} is the terminal velocity (m s^{-1}), $a_R = 141.5$, the Gamma function $\Gamma(4.5) = 11.63$, $\rho_w = 1000 \text{ kg m}^{-3}$ is the density of water, ρ_a (kg m^{-3}) is the air density and

$$\lambda_R = \left(\frac{\pi \rho_w N_{R0}}{\rho q_R} \right)^{1/4} \quad (4.23)$$

and $N_{R0} = 8 \times 10^6$ and q_R (kg kg^{-1}) is the cloud rain mixing ratio.

If rainfall is present in the lowest layer of the CTM then the wet deposition velocity V_{wet} (m s^{-1}) is calculated as follows.

$$V_{wet} = \frac{\rho_a}{\rho_w} V_{TR} q_R \quad (4.24)$$

The wet deposition flux is then given by $V_{wet} C$, where C is the species concentration in the lowest level of the model.

5. CHEMICAL TRANSFORMATION

5.1 Method of solution

Chemical transformation is modelled by the CTM as a coupled system which includes the processes of vertical diffusion, dry deposition and mass emissions. The governing equation (in a Cartesian coordinate system) for the i^{th} reacting species is given by

$$\frac{\partial C_i}{\partial t} = \frac{\partial}{\partial z} \rho_a K_z \frac{\partial C_i / \rho_a}{\partial z} + R_i + S_i \quad (5.1)$$

where C_i is the concentration of the i^{th} species, S_i is the source rate of the i^{th} species (including emissions and chemical transformation), and R_i is the removal rate of the i^{th} species (from chemical transformation).

Eqn (5.1) is solved with the boundary conditions:

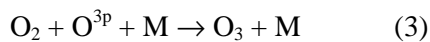
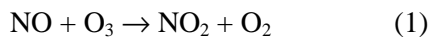
$K_z \frac{\partial C_i / \rho_a}{\partial z} = 0$ at the top boundary; and $K_z \frac{\partial C_i}{\partial z} = -V_{dry,i} C_i$ at the surface; and $C_i = C_0$ at $t = t_0$ where C_0 is the initial concentration.

The solution proceeds by re-casting eqn (5.1) into the following form.

$$\frac{\partial C_i}{\partial t} = F_i - L_i C_i \quad (5.2)$$

where F_i is the formation rate and L_i is the loss rate for the i^{th} species.

As an example, we consider the following simple chemical system



If we define the rate coefficients for reactions 1–3 as k_1 , k_2 , and k_3 respectively then the rate of change of NO_2 will be given by

$$\frac{d[\text{NO}_2]}{dt} = k_1[\text{NO}][\text{O}_3] - k_2[\text{NO}_2] \quad (5.3)$$

Comparing eqn (5.2) and eqn (5.3) shows that the formation and loss rates for nitrogen dioxide will be given by the following.

$$F_{\text{NO}_2} = k_1[\text{NO}][\text{O}_3], \text{ and } L_{\text{NO}_2} = k_2 .$$

The vertical diffusion is expressed in the form of eqn (5.2) by first spatially discretising the diffusion component of eqn (5.1) as follows (for constant thickness layers).

$$\frac{dC_{i,k}}{dt} = \frac{1}{\Delta z_k^2} \left(\frac{\rho_{a,k+1/2}}{\rho_{a,k+1}} K_{z,k+1/2} C_{i,k+1} + \frac{\rho_{a,k-1/2}}{\rho_{a,k-1}} K_{z,k-1/2} C_{i,k-1} \right) - \left[\frac{1}{\Delta z_k^2} \left(\frac{\rho_{a,k+1/2}}{\rho_{a,k}} K_{z,k+1/2} + \frac{\rho_{a,k-1/2}}{\rho_{a,k}} K_{z,k-1/2} \right) \right] C_{i,k} \quad (5.4)$$

Note that here the indice k refers to the vertical level while the indice i again refers to the i^{th} species. It can be seen that eqn (5.4) has an equivalent form to that shown in eqn (5.2) with the first term on the right hand side being equivalent to F_i and the second term being equivalent to L_i .

This set of coupled nonlinear ordinary differential equations is solved by a modified version of a hybrid predictor-corrector method originally used in the Carnegie Mellon, California Institute of Technology airshed model (McRae et al., 1982). The solution procedure uses a combination of semi-implicit and explicit solvers which are applied by dynamically dividing the system into stiffness categories estimated from the loss rate (i.e. how quickly C_i reaches equilibrium). An adaptive time step is used and solution proceeds until the integration covers a full advection time step.

For each chemistry time step Δt_c the model performs an iterative predictor-corrector sequence to generate an updated concentration of each species, C_i . The predictor-corrector solver is determined dynamically by the loss rate τ_i , and is given by eqn (5.6) where n represents the current time step, $n+1$ represents the end of the timestep i.e. $t_{n+1}=t_n+\Delta t$ and * represents an intermediate value from the prediction equation to be used in the subsequent correction equation.

$$\tau_i > \Delta t \quad \text{:slow} \quad (5.5a)$$

$$\tau_i \leq \Delta t \quad \text{:stiff (short-lived)} \quad (5.5b)$$

$$\tau_i \ll \Delta t \quad \text{:fast} \quad (5.5c)$$

where, $\tau_i = 1/L_i$

The solution procedures are as follows.

- Slow

Predictor:

$$C_i^* = C_i^n + \Delta t_c (F_i^n - L_i^n C_i^n) \quad (5.6a)$$

Corrector:

$$C_i^{n+1} = C_i^n + \frac{\Delta t_c}{2} (F_i^n - L_i^n C_i^n + F_i^* - L_i^* C_i^*) \quad (5.6b)$$

- Stiff;

Predictor:

$$C_i^* = \frac{C_i^n (2\tau_i^n - \Delta t_c) + 2F_i^n \tau_i^n \Delta t_c}{2\tau_i^n - \Delta t_c} \quad (5.6c)$$

Corrector:

$$C_i^{n+1} = \frac{C_i^n (\tau_i^n + \tau_i^* - \Delta t_c) + (\Delta t_c / 2) (F_i^n + F_i^*) (\tau_i^n + \tau_i^*)}{\tau_i^n + \tau_i^* + \Delta t_c} \quad (5.6d)$$

- Fast

Predictor:

$$C_i^* = \frac{F_i^*}{L_i^n} \quad (5.6e)$$

Corrector:

$$C_i^{n+1} = \frac{F_i^*}{L_i^*} \quad (5.6f)$$

The initial time step is estimated using species whose concentrations are greater than a lower bound concentration threshold. This is done to avoid time spent tracking species which are present only at very low concentrations and thus are not strongly coupled into the chemical system.

$$\Delta t_{c,0} = \max \left(\Delta t_{c,\min}, \min \left[\Delta t_{c,\max}, \alpha \cdot \Delta t_{diff}, \left(\frac{\beta C_i}{F_i - LC_i} \right) \right] \right) \quad (5.7)$$

where Δt_{diff} is a Courant-limited maximum time step for the vertical diffusion

$$(\Delta t_{diff} = 0.5 \Delta z^2 / K_z)$$

and,

α is a scaling factor which by default is $1/3$.

β is the maximum allowable percentage change in species concentration (typically 1×10^{-3}).

$\Delta t_{c,\min}$ is a specified minimum initial time step (1×10^{-5} s).

$\Delta t_{c,\max}$ is a specified maximum initial time step (set to the advection time step).

For a photochemical system the lower bound concentration is taken as 0.1% of the composite consumption rate given by $C_{comp} = C_{NO} + C_{NO_2} + C_{O_3}$. For a tracer or aerosol system the cut-off is taken as 0.1% of the total sum of the constituents.

The integration process occurs as follows.

1. The initial time step is calculated using eqn (5.7).
2. The solution is then advanced through a predictor-corrector cycle using the solvers given in eqn (5.6).
3. The relative error norm is calculated and the solution is considered to have converged if the error $\epsilon < 0.001$.
4. If the solution hasn't converged after 10 iterations of corrector then the time step is reduced by a factor of 0.7.
5. If the solution converges within 3 iterations then the time step is increased by a factor of 1.1.
6. If the time step is increased three or more times in a row then the minimum starting time step is set to a lower bound of 1 s.

To facilitate the solution process, species can optionally be lumped together into species families (Mathur 1998). This process is used to reduce the stiffness of the chemical mechanism by representing linear combinations of species that either exhibit strong coupling or ensuring mass balance for a conservative grouping such as total nitrogen. Following the solution of each lumped species, the individual species can be appropriately scaled or adjusted directly from the lumped equations.

5.2 The CTM chemical compiler

The CTM has been designed to enable different photochemical transformation mechanisms to be readily implemented into the model using a chemical compiler. The compiler uses a text-based description of a chemical transformation mechanism to generate a series of software modules which can be compiled and linked with the CTM executable code.

By way of example, Figure 4 shows part of a text-based description for the Generic Reaction Set (Azzi et al. 1992), a highly condensed photochemical smog mechanism. It can be seen that the description includes tables of species definitions and reactions. The species definition table includes a species name mnemonic (case sensitive); a species description; a flag to indicate whether the species is transported and integrated using the chemical solver; or treated as steady-state and generated during the call to the chemical solver and solved using an analytic or numerical solution generated by the compiler (SS). In the case of the latter, the compiler attempts to generate and write a software description for one of the following seven analytic or numerical solutions.

1. Linear independent (not a function of other steady state species)- analytic solution.
2. Quadratic independent (not a function of other steady state species)- analytic solution.
3. Linear dependent (also a function of other linear independent steady state species)- analytic solution.
4. Quadratic dependent (also a function of other linear independent or quadratic independent steady state species)- analytic solution.
5. Non-linear (third order steady state species)- solved by linear iteration.

6. Non-linear quadratic (quadratic with other non-linear steady state terms)- solved by linear iteration.

7. Second order species- solved by linear iteration.

The remainder of the species definition table lists whether the species is a gas or an aerosol, the species molecular weight, concentration bounds and surface uptake resistances (see section 4.1).

A description of the chemical transformation reactions follows the species definitions. It can be seen that each row lists the reactants and products of a reaction, a rate coefficient definition and a series of related parameters which are specific for each reaction. Table 2 provides a description of the 13 rate coefficients which are treated by the chemical compiler and Table 3 lists the 22 photolysis reactions which are currently defined by the compiler.

```

!-----
!CHEM PROCESSOR TEXT FILE
!-----
grs
v1.0b
!-----
!SPECIES NAMES AND DESCRIPTION
! short name, long name, de/ss/lp/nr, g/a, mw (g), min Conc (ppb|ug/m3), Rsoil (s/m), Rwater, Rurban
!-----
StartSpecies
SO2 , 'sulfur dioxide'           ,DE,g,64.1,1.0e-10,1000 , 0.0 ,400
NO  , 'nitric oxide'            ,DE,g,30.0,1.0e-10, 10000,10000,10000
NO2 , 'nitrogen dioxide'        ,DE,g,46.0,1.0e-10, 500 ,1500 ,500
ROC , 'reactive organic carbon' ,DE,g,13.7,1.0e-10,1.0E10,1.0E10,1.0E10
RP  , 'radical product'         ,SS,g,33.0,1.0e-15,1.0E10,1.0E10,1.0E10
!
O3  , 'ozone'                   ,DE,g,48.0,1.0e-10,400 ,20000 ,400
SGN , 'stable gaseous nitrate'   ,DE,g,63.0,1.0e-10,10 ,10 ,10
SNGN,'stable gaseous nitrate'   ,DE,g,63.0,1.0e-10,10 ,10 ,10
NOx , 'oxides of nitrogen'      ,LP,g,DIFF,4, NO,1,NO2,1,SGN,1,SNGN,1
EndSpecies
!-----
!REACTION MECHANISM DESCRIPTION.
!REACTION, REACTION TYPE, TYPE PARAMETERS
!-----
StartReaction
ROC => ROC + RP ; GRS1 ; 1.0, -4700., 0.00316
NO + RP => NO2 ; CONS ; 8.1259E-12
NO2 => NO + O3 ; PHOT ; 1,1.0
NO + O3 => NO2 ; ARRH ; 2.0973E-12,-1450.
RP + RP => RP ; CONS ; 6.764E-12
NO2 + RP => SGN ; CONS ; 8.1168E-14
NO2 + RP => SNGN ; CONS ; 8.1168E-14
EndReaction
!-----
!SPECIES CLASSIFIED AS NOX [for emission
! AS ROC [scaling in
! AS PM [the CTM]
! 0 = no species in this precursor category
!-----
StartEmissionScaling
2,NO,NO2
1,ROC

```

Figure 4 Example of the text-based input used by the chemical compiler to build a software description of a chemical transformation mechanism for use by the CTM.

Table 2 Description of the rate coefficient function used by the CTM chemical compiler.

Key	Description	Variable						
		1	2	3	4	5	6	7
ARRH	Arrhenius. $k = Ae^{\left(\frac{-B}{T}\right)}$	A	B					
PHOT	$k = f \bullet J_i$ (see photolysis look-up table)	<i>i</i>	<i>f</i>					
TROE	<p>Troe falloff reaction</p> $k = \frac{k_0[M]}{1 + k_0[M]/k_\infty} F_c^{\{1+[N^{-1} \log(k_0[M]/k_\infty)]^2\}^{-1}};$ $k_0 = S_1 \left(\frac{T}{300}\right)^{S_2}; k_\infty = S_3 \left(\frac{T}{300}\right)^{S_4};$ $F_c = S_5; N = 1.0$	S ₁	S ₂	S ₃	S ₄	S ₅		

Key	Description	Variable						
EQUI	Reverse equilibria form $k = \frac{k_0[M]}{1 + k_0[M]/k_\infty} F_c^{\{1+[N^{-1} \log(k_0[M]/k_\infty)]^2\}^{-1}}$ $k = k_{troe} A \exp\left(\frac{-B}{T}\right)$ $k_0 = S_1 \left(\frac{T}{300}\right)^{S_2}; k_\infty = S_3 \left(\frac{T}{300}\right)^{S_4}$ $F_c = S_5; N = 1.0$	as above	as above	as above	as above	A	B	S ₇
FALL	Extended Troe fall-off expression $k = \frac{k_0[M]}{1 + k_0[M]/k_\infty} F_c^{\{1+[N^{-1} \log(k_0[M]/k_\infty)]^2\}^{-1}}$ $k_0 = S_1 \left(\frac{T}{300}\right)^{S_2} e^{\frac{-S_3}{T}}; k_\infty = S_4 \left(\frac{T}{300}\right)^{S_5} e^{\frac{-S_6}{T}}$ $F_c = S_7; N = 1.0$	S ₁	S ₂	S ₃	S ₄	S ₅	S ₆	S ₇
CONS	$k = C$	C						
GRS1	GRS mechanism $k = J_{no2} e^{A\left(\frac{1}{T} - \frac{1}{T_r}\right)}$	i	A	$\frac{1}{T_r}$				

CHEMICAL TRANSFORMATION

Key	Description	Variable						
TDAF	$J_{no2} = J_i$ (i=1, see photolysis look-up table) Arrhenius with a temperature dependent A factor $k = A(T)e^{\left(\frac{-B}{T}\right)}$ $A(T) = A_1T^{A_2}$	A ₁	A ₂	B				
ARRW	Weighted Arrhenius reaction $k = W_1A_1e^{\left(\frac{-B_1}{T}\right)} + W_2A_2e^{\left(\frac{-B_2}{T}\right)}$	W ₁	A ₁	B ₁	W ₂	A ₂	B ₂	
ARRM	Third-body weighted Arrhenius $k = A_1e^{\left(\frac{-B_1}{T}\right)} + A_2e^{\left(\frac{-B_2}{T}\right)} \times [M]$	A ₁	B ₁	A ₂	B ₂			
LMHW	Lindemann-Hinshelwood reaction $k = k_0 + \left(\frac{k_3[M]}{1 + k_3[M]/k_2} \right)$	A ₁	B ₁	A ₂	B ₂	A ₃	B ₃	

Key	Description	Variable					
SPRS	$k_0 = A_1 e^{\left(\frac{-B_1}{T}\right)}$ $k_2 = A_2 e^{\left(\frac{-B_2}{T}\right)}$ $k_3 = A_3 e^{\left(\frac{-B_3}{T}\right)}$ <p>Scaled pressure reaction</p> $k = A(T)(1.0 + 0.6P)$ $A(T) = A_1 \left(\frac{T}{300}\right)^{A_2}$	A ₁	A ₂				
TDCN	<p>Constant rate with temperature dep</p> $A(T) = A_1 \left(\frac{T}{300}\right)^{A_2}$	A ₁	A ₂				

Table 3 The photolysis rates treated by the chemical compiler.

Map	Reaction	Description
1	$\text{NO}_2 \rightarrow \text{NO} + \text{O}(3\text{P})$	Nitrogen Dioxide photolysis
2	$\text{O}_3 \rightarrow \text{O}^1\text{D}$	Ozone photolysis to O^1D
3	$\text{HCHO} \rightarrow \text{H} + \text{HCO}$	Formaldehyde photolysis to radicals
4	$\text{HCHO} \rightarrow \text{H}_2 + \text{CO}$	Formaldehyde photolysis to H_2
5	$\text{CH}_3\text{CHO} \rightarrow \text{CH}_3\text{OO} + \text{CO} + \text{HO}_2$	Acetaldehyde photolysis
6	ISPD \rightarrow prods	Isoprene products (legacy only)
7	$\text{CH}_3\text{COC}_2\text{H}_5 \rightarrow \text{CH}_3\text{CHO} + \text{prods}$	Methyl Ethyl Ketone photolysis
8	$\text{NO}_3 \rightarrow \text{NO} + \text{O}_2$	Nitrate photolysis to NO
9	$\text{HCOCH}=\text{CHCHO} \rightarrow 0.98 \text{HO}_2 + \text{prods}$	Dicarbonyl photolysis
10	$\text{O}_3 \rightarrow \text{O}^1\text{P}$	Ozone photolysis to O^3P
11	$\text{NO}_3 \rightarrow \text{NO}_2 + \text{O}^3\text{P}$	Nitrate photolysis to NO_2
12	$\text{HONO} \rightarrow \text{NO} + \text{OH}$	Nitrous acid photolysis
13	$\text{H}_2\text{O}_2 \rightarrow \text{OH} + \text{OH}$	Hydrogen peroxide photolysis
14	$\text{HNO}_4 \rightarrow \text{HO}_2 + \text{NO}_2$	Pernitric acid photolysis
15	$\text{HNO}_3 \rightarrow \text{OH} + \text{NO}_2$	Nitric acid photolysis
16	$\text{N}_2\text{O}_5 \rightarrow \text{NO}_2 + \text{NO}_3$	Dinitrogen pentoxide photolysis
17	$\text{CH}_3\text{ONO}_2 \rightarrow \text{products}$	Organic nitrate photolysis (NTR)
18	ROOH \rightarrow products	Higher organic peroxide photolysis
19	$\text{PAN} \rightarrow \text{C}_2\text{O}_3$	Peroxy acetyl nitrate photolysis
20	$\text{C}_2\text{CHO} \rightarrow \text{CH}_3\text{OO} + \text{CO} + \text{HO}_2$	Propionaldehyde photolysis
21	$\text{CH}_3\text{COCHO} \rightarrow \text{C}_2\text{O}_3 + \text{HO}_2 + \text{CO}$	Methyl glyoxal photolysis
22	$\text{C}_3\text{H}_4\text{O} \rightarrow \text{prods}$	Acrolein photolysis

5.3 Chemical transformation mechanisms

The CTM chemical compiler has been used to generate seven core chemical systems which are available for use by the CTM. The chemical systems are summarised in Table 4 and a detailed listing of each mechanism is given in the Appendix.

Table 4 Summary of the chemical mechanisms generated by the CTM chemical compiler.

Key	Mechanism	Description
NOX	NO, NO ₂	Simple two species tracer mechanism used for testing and training. Links to an urban photochemical precursor inventory.
OX	NO, NO ₂ , O ₃	Models the photochemical steady-state system. Used for testing and training. Links to an urban photochemical precursor inventory
HG3t	Three species mercury tracer mechanism	Models the transport and deposition of elemental, bi-valent and particulate mercury. No chemical reactions
GRS	Generic Reaction Set (Azzi et al. 1992)	Highly condensed photochemical transformation mechanism. Using for training and screening-level urban ozone modelling. Links to an urban photochemical precursor inventory however requires a correctly defined reactivity-weighted volatile organic compound.
LCC	Lurmann, Carter, Coyner mechanism (Lurmann et al. 1987)	Lumped species photochemical smog mechanism which has seen wide use in Australia and the U.S. Links to an urban and regional photochemical precursor inventory however requires correctly speciated VOC emissions.
CB05	Carbon Bond 2005 (Yarwood et al. 2005)	Lumped and structure photochemical smog mechanism which as recently been implemented into U.S models and the CTM. Links to urban and regional photochemical precursor inventories however requires correctly speciated VOC emissions.
CB05_AER	Carbon Bond 2005 + aerosol species	The version of the mechanism contains addition species and reactions for modelling the primary and secondary production of PM _{2.5}

6. AEROSOL PROCESSES

The CTM contains a mass-based scheme for modelling primary and secondary aerosols. The CTM has been used for modelling wind blown dust, smoke and primary urban particles as part of the Australian Air Quality Forecasting System (Cope et al. 2004). Additionally the CTM has been used for modelling primary and secondary particles from urban and natural sources (Cope et al. 2009). The CB05_AER chemical scheme caters for primary and secondary aerosols in the fine ($< 2.5 \mu\text{m}$) and coarse ($2.5\text{--}10 \mu\text{m}$) size fractions from urban sources (as elemental carbon, organic carbon, sulfate); from sea salt (see section 7.2.5) and from secondary inorganic (section 6.1) and organic (section 6.2) particle production. A description of the secondary particle generation schemes now follows. Section 7 includes a description of the sea salt and wind blown dust algorithms and a complete listing of the aerosol species contained in the CB05_AER mechanism are given in section 7 of the Appendix.

6.1 Secondary inorganic aerosol mechanisms

Secondary inorganic aerosol production is modelled using a thermodynamic equilibrium approach. The research version of the CTM has the option of using either the Model for an Aerosol Reacting System [MARS, Saxena et al. (1985)] or ISORROPIA (Nenes et al. 1998). The ISORROPIA model is not available in the commercial version of the CTM. Both models use computationally efficient methodologies to predict the composition of water and multiphase aerosols (see Table 5).

MARS simulates an ammonium, sulfate, nitrate and water system. The aerosol composition is driven by the total ambient concentrations of H_2SO_4 , HNO_3 , NH_3 , H_2O and temperature. Separate liquid and solid aerosol phases are treated by MARS. Different algorithms are used depending upon whether the modelled ambient environment is ammonia-rich ($[\text{NH}_3] > 2[\text{H}_2\text{SO}_4]$) or ammonia lean. In the case of the former three sub-categories are also defined on the basis of high relative humidity ($\geq 80\%$), medium ($62\% \leq \text{humidity} < 80\%$) and low relative humidity ($< 62\%$). This approach enables a reduced number of equations to be considered in each regime with a concurrent reduction in computational overheads. A complete description of the MARS mechanism is given in Saxena et al. (1985).

Table 5. Gas and aerosol phase species included in the MARS and ISORROPIA models

Phase		
Gas	Aqueous	Solid
H ₂ SO ₄ , NH ₃ ,	SO ₄ ²⁻ , HSO ₄ ⁻ ,	(NH ₄) ₂ SO ₄ , (NH ₄) ₃ H(SO ₄) ₂ ,
HNO ₃ , H ₂ O	NH ₄ ⁺ , NO ₃ ⁻ , H ⁺ , OH ⁻ H ₂ O(l)	NH ₄ HSO ₄ , NH ₄ NO ₃
Additional species modelled by ISORROPIA		
HCL	CL ⁻	NH ₄ CL, NaCL, NaNO ₃ , NaHSO ₄ , Na ₂ SO ₄

ISORROPIA can model a sodium, ammonium, chloride, sulfate, nitrate and water aerosol system (see Table 5). Equilibrium aerosol concentrations are generated by minimising the total Gibbs free energy of the aerosol system, an approach which enables the deliquescence relative humidity to be modelled for a mixed salt system. A description of ISORROPIA is given in Nenes et al. (1998) and Ansari and Pandis (1999).

Table 10 lists the species which have been added to the core Carbon Bond 2005 mechanism to drive MARS and ISORROPIA. Note that this version of the mechanism does not explicitly include sodium and chloride (i.e. as separate components of sea salt) and thus ISORROPIA is limited to modelling aerosol sulfate and nitrate with this version of Carbon Bond.

6.2 The secondary organic aerosol mechanism

The CTM secondary organic aerosol (SOA) module is based on the semi-empirical absorptive partitioning model (Odum et al. 1996) in which semi-volatile products are generated from the oxidation of parent VOC species and partitioned between the gas and aerosol phases. The partitioning is treated as a dynamical equilibrium absorptive process in which the condensing aerosol is partitioned into the aerosol bulk liquid phase by Raoult's law (Pun and Seigneur

2007) and reacts instantaneously to changes in temperature, concentration of the semi-volatile product and mass of the absorbing aerosol phase.

Following Odum et al. (1996), the yield Y of a VOC is defined as the ratio of the mass of SOA formed (ΔM_{om}) to the mass of parent species reacted (ΔVOC).

$$Y = \frac{\Delta M_{om}}{\Delta VOC} = M_{om} \sum_{i=1}^n \alpha_i K_{om,i} / (1 + K_{om,i} M_{om}) \quad (6.1)$$

Here M_{om} is the absorbing organic aerosol mass concentration ($\mu\text{g}/\text{m}^3$), $K_{om,i}$ is the partitioning coefficient ($\mu\text{g}/\text{m}^3$)⁻¹ between the gas and aerosol phases, and α_i is a stoichiometric ratio that relates the amount of condensable product generated to the amount of parent VOC consumed. The product yields and partitioning coefficients are determined empirically from environmental smog chamber studies.

For a given value of $K_{om,i}$ and M_{om} , the partitioning of the condensable product between the gaseous and aerosol phases is described as follows (Pun et al., 2006).

$$A_{om,i} = \frac{CG_i M_{om} K_{om,i}}{(1 + K_{om,i} M_{om})} \quad (6.2),$$

where A ($\mu\text{g}/\text{m}^3$) is the mass of condensable product existing in the aerosol phase and CG is the total amount of condensable product available for partitioning. It then follows that $G_i = CG_i - A_{om,i}$ is the mass of condensable product existing in the gas phase and the partitioning coefficient may be expressed as follows.

$$K_{om,i} = A_{om,i} / (G_i M_{om}) \quad (6.3)$$

The SOA yield is observed to vary with ambient temperature (Takekawa et al. 2003), with higher yields observed at lower temperatures. If a Raoult's law partitioning is assumed then the temperature dependency of the partitioning coefficient may be described as follows (Pankow 1994, Takekawa et al. 2003).

$$K_{om,i} = K_{298,i} \frac{T}{298} \exp \left[\frac{\Delta H_{vap,i}}{R} \left(\frac{1}{T} - \frac{1}{298} \right) \right] \quad (6.4)$$

where $K_{298,i}$ is the partitioning coefficient measured at $T = 298\text{K}$; $\Delta H_{vap,i}$ is the enthalpy of vaporisation (72700 J M^{-1} Pun et al. 2006) and R is the ideal gas constant ($8.206 \times 10^{-5} \text{ m}^3 \text{ atm mol}^{-1} \text{ K}^{-1}$).

The module includes a very simple parameterisation for the formation of non-volatile SOA oligomers (Morris et al. 2006).

$$\frac{dA_{olig}}{dt} = \frac{1}{\tau_{olig}} \sum_{i=1}^{nso} A_{om,i} \quad (6.5)$$

where A_{olig} is the mass of SOA oligomer, τ_{olig} is the oligomerisation time scale ($\tau_{olig} = 28.85 \text{ h}$; which gives a 50% conversion of A_{om} to non-volatile oligomers after 20 hours; Morris et al. 2006).

The SOA module also includes a simplified version of the methodology discussed in Pun and Seigneur (2007) for investigating the sensitivity of aerosol yield to aerosol liquid water content (LWC $\mu\text{g}/\text{m}^3$). For a semi-condensable species that is assumed to partition into an organic–water phase according to Raoult’s law, aerosol water plays two roles in mediating the partitioning of the condensable product between the gaseous and aerosol phases. Firstly, a change in the aerosol liquid water content leads to a proportional change in the mass of the absorbing organic-aerosol phase and hence the partitioning of the condensable product between the gas and aerosol phases via eqn (6.2). Secondly, the presence of aerosol water changes the partitioning coefficient because the magnitude of $K_{om,i}$ varies inversely with the mean molecular weight \bar{M}_{om} of the absorbing phase (Pankow 1994). Thus $K_{om,i} \propto \bar{M}_{om}^{-1}$ and $K_{om,i}$ will be increased for large SOA molecules and polymers as the liquid water content of the solvent is increased because the mean molecular weight will be reduced by the presence of water.

The CTM secondary organic aerosol module uses eqn (6.2) to model the formation of SOA from six hydrocarbon precursor groups- olefins, paraffin’s, xylene’s, toluene, terpenes and isoprene the module uses the stoichiometric and partitioning coefficients recommended by Singh et al. (2007) and Pun and Seigneur (2007). Note however that the stoichiometric coefficients for the olefin and paraffin reactions have been modified from those recommended by Singh et al. (2007) in order to represent only the long chain fraction of the lumped species used by Carbon Bond 2005. This was done using the molar fractions of C8+ paraffin in the paraffin emissions and similarly for the olefin emission specified in the Melbourne (Australia)

air emissions inventory. These fractions were found to be 3.3% and 1.4% respectively of the total emissions for each species group.

The gas phase reactions and the condensable products are documented in Table 6, and the gas-aerosol equilibrium reactions are shown in Table 7. The condensable products and SOA species are included in the CB05_AER mechanism.

6.2.1 Method of solution

The steady-state SOA aerosol mass (eqn 6.2) has to be solved for the 13 species system listed in Table 7. However the problem is non-linear because the absorbing aerosol mass (M_{om}) includes $A_{om,i}$, and thus the equilibrium masses for the SOA system has to be solved by iteration. An efficient method for solving the system can be derived by noting that an analytic solution exists for the case of a one-species system. This can be seen by setting $M_{om} = M'_{om} + A_{om,i}$; where M'_{om} is the non-volatile component of the absorbing aerosol mass (given by the primary organic aerosol mass + the oligomerised SOA mass). Solving eqn (6.2) using M'_{om} in place of M_{om} gives the following result.

$$A_{om} = \frac{-b + \sqrt{b^2 - 4ac}}{2a} \quad (6.6)$$

where $a = K_{om}$; $b = 1 + K_{om}(M'_{om} - C_t)$; $c = -K_{om}M'_{om}C_t$

and $C_t = A_{om} + CG$ is the total species mass available for partitioning between the aerosol and gaseous phases.

Taking the quadratic analytic solution and applying it in a linear iteration algorithm for the 13 SOA species provides a solution methodology which is fast and stable provided that the adsorbing mass is not small compared to the condensing aerosol mass. Given this the solution methodology is as follows.

1. Add up the non-volatile organic mass and SOA mass from the previous time step to generate a first guess of the adsorbing mass.
2. Using eqn 6.6, calculate an updated SOA mass for each of the 13 SOA species.
3. Generate a new absorbing mass and repeat until the SOA mass change becomes small.

Table 6 Semi-condensable aerosol forming reactions for VOC precursor compounds

Surrogate Precursor Compound	Gas-Phase Reactions ¹ and Stoichiometry	Rate Constants (cm ³ molec ⁻¹ s ⁻¹)
Straight chain olefins	OLE + OH → 0.0001 CG1 + 0.0149 CG2	3.2 x 10 ⁻¹¹
Straight chain paraffins	PAR + OH → 0.0018 CG3	8.1 x 10 ⁻¹³
Xylene and other low SOA yield aromatics	XYL + OH → 0.023 CG4 + 0.046 CG5	2.0 x 10 ⁻¹¹ exp (116/T)
Toluene and other high SOA yield aromatics	TOL + OH → 0.033 CG6 + 0.083 CG7	1.8 x 10 ⁻¹² exp (355/T)
α-Pinene as a surrogate for terpenes	TERP + OH → 0.028 CG8 + 0.061 CG9	1.5 x 10 ⁻¹¹ exp (449/T)
	TERP + O ₃ → 0.089 CG10 + 0.033 CG11	1.2 x 10 ⁻¹⁵ exp (-821/T)
Isoprene	ISOP + OH → 0.232 CG12 + 0.0288 CG13	2.54 x 10 ⁻¹¹ exp(407.6/T)

¹Showing only the condensable species.

Table 7 Aerosol forming equilibria for SOA compounds

Secondary organic aerosol compound	Equilibrium reaction	Equilibrium constants (dry and at 298 °K)
SOLE1	CG1 ↔ SOLE1	1.0
SOLE2	CG2 ↔ SOLE2	0.005
SPAR	CG3 ↔ SPAR	0.044
SXYL1	CG4 ↔ SXYL1	0.13
SXYL2	CG5 ↔ SXYL2	0.0042
STOL1	CG6 ↔ STOL1	0.16
STOL2	CG7 ↔ STOL2	0.0057
STER1	CG8 ↔ STER1	0.51
STER2	CG9 ↔ STER2	0.012
STER3	CG10 ↔ STER3	0.26
STER4	CG11 ↔ STER4	0.24
SISO1	CG12 ↔ SISO1	0.00862
SISO2	CG13 ↔ SISO2	1.62

The Carbon Bond core and extension species required by the SOA mechanism are shown in Table 8.

Table 8 Core and extension species used by Carbon Bond 2005 for modelling secondary organic production.

Species CB05 name	Description	Molecular weight
O3	Ozone	48.0
OH	Hydroxyl radical	64.1
OLE	Terminal olefin bond	28.0
ISOP	Isoprene	68.1
TERP	Terpene	136.0
TOL	Toluene an monoalkyl aromatics	92.0
XYL	Xylene and polyalkyl aromatics	106.0
PAR	Paraffin	14.3
OC25	PM2.5 primary organic carbon aerosol	aerosol
CG1	OLE condensable gas #1	140
CG2	OLE condensable gas #2	140
CG3	PAR condensable gas	140
CG4	XYL condensable gas #1	150
CG5	XYL condensable gas #2	150
CG6	TOL condensable gas #1	150
CG7	TOL condensable gas #2	150
CG8	TERP condensable gas #1	184

AEROSOL PROCESSES

Species CB05 name	Description	Molecular weight
CG9	TERP condensable gas #2	184
CG10	TERP condensable gas #3	184
CG11	TERP condensable gas #4	184
CG12	ISO condensable gas #1	150
CG13	ISO condensable gas #2	150
SOL1	Olefin SOA #1	aerosol
SOL2	Olefin SOA #2	aerosol
SPAR	Paraffin SOA	aerosol
SXY1	Xylene SOA #1	aerosol
SXY2	Xylene SOA #2	aerosol
STOL1	Toluene SOA #1	aerosol
STOL2	Toluene SOA #2	aerosol
STE1	Terpene SOA #1	aerosol
STE2	Terpene SOA #2	aerosol
STE3	Terpene SOA #3	aerosol
STE4	Terpene SOA #4	aerosol
SIS1	Isoprene SOA #1	aerosol
SIS2	Isoprene SOA #2	aerosol
NSOA	SOA oligomer	aerosol

6.3 In-cloud sulphate production

The CTM includes a bulk scheme for modelling sulphate S(VI) production within cloud water and cloud rain. The scheme is a simplified version of that presented in Seinfeld and Pandis (1998, Section 6.5) and considers the production of S(VI) from the reaction of S(IV) with aqueous phase ozone and hydrogen peroxide.

In the case of S(IV) oxidation by ozone is given as follows,



where the rate expression is given by (Hoffmann and Calvert 1985)

$$R_{\text{O}_3} = -\frac{d[\text{S(IV)}]}{dt} = (k_0[\text{SO}_2(\text{aq})] + k_1[\text{HSO}_3^-] + k_2[\text{SO}_3^{2-}])[\text{O}_3(\text{aq})] \quad (6.7b)$$

and

$$k_0 = 2.4 \times 10^4 \text{ M}^{-1} \text{ s}^{-1}; k_1 = 3.70 \times 10^5 \exp(-5530/T) \text{ M}^{-1} \text{ s}^{-1}; \text{ and}$$

$$k_2 = 1.5 \times 10^9 \exp(-5280/T) \text{ M}^{-1} \text{ s}^{-1};$$

For hydrogen peroxide,



and the rate expression is again given by Hoffmann and Calvert (1985).

$$R_{\text{H}_2\text{O}_2} = -\frac{d[\text{S(IV)}]}{dt} = \frac{k[\text{H}^+][\text{H}_2\text{O}_2(\text{aq})][\text{HSO}_3^-]}{1 + K[\text{H}^+]} \quad (6.8b)$$

and

$$k = 7.5 \times 10^7 \exp(-4430/T) \text{ M}^{-1} \text{ s}^{-1}; \text{ and } K = 13 \text{ M}^{-1}. \quad (6.9)$$

The dissolved concentrations of O_3 and H_2O_2 are derived from their partial pressures in the cloud air and their Henry's law coefficients for a closed cloud air- cloud water.

$$[\text{O}_3(\text{aq})] = \frac{H_{\text{O}_3} p_{\text{O}_3}^0}{1 + 10^6 \text{LRTH}_{\text{O}_3}} \quad (6.10a)$$

and

$$[\text{H}_2\text{O}_2(\text{aq})] = \frac{H_{\text{H}_2\text{O}_2} p_{\text{H}_2\text{O}_2}^0}{1 + 10^6 \text{LRTH}_{\text{H}_2\text{O}_2}} \quad (6.10b)$$

where H_{O_3} and $H_{\text{H}_2\text{O}_2}$ are the Henry's law constants for O_3 and H_2O_2 respectively (see Table 9); $p_{\text{O}_3}^0$ and $p_{\text{H}_2\text{O}_2}^0$ (mb) are the partial pressures prior to dissolution in the cloud water; L is the liquid water content (here g m^{-3}) which is provided by the host meteorological model; $R = 0.08205$ ($\text{atm L mol}^{-1} \text{K}^{-1}$) is the ideal gas constant; and T (K) is the ambient temperature.

6.3.1 Aqueous-Phase Chemical Equilibria

The rate expressions in eqn (6.7) and eqn (6.8) require the concentrations of the bi-sulfite ion (HSO_3^-), the sulfite ion (SO_3^{2-}) and the hydrogen ion (H^+). In the CTM these are derived for a cloud air/water system which contains carbon dioxide (CO_2), sulphur dioxide (SO_2), O_3 , H_2O_2 , ammonia (NH_3), nitric acid (HNO_3) and their associated aqueous phase dissolution species and disassociated ionic products.

Table 9 lists the equilibrium reactions which are considered in the aqueous phase chemical mechanism. Note that reactions of the form $\text{A} + \text{H}_2\text{O} \leftrightarrow \text{A}(\text{aq})$ have an equilibrium constant which is equivalent to the Henry's law coefficient, where $\text{A}(\text{g})$ is expressed as a partial pressure (atm), $\text{A}(\text{aq})$ is expressed in units of mol l^{-1} (M) and $\text{A}(\text{aq}) = H_{\text{A}}\text{A}(\text{g})$ and H_{A} is the Henry's law coefficient. In the case of aqueous phase equilibria, the equilibrium constants K_{A} are expressed in units of M.

The temperature dependence of the equilibria reactions are treated using the van't Hoff equation.

$$K_{\text{A}}(T) = K_{\text{A}}(298) \exp \left[-\frac{\Delta H_{\text{A}}}{R} \left(\frac{1}{T} - \frac{1}{298} \right) \right] \quad (6.11)$$

Where T is the temperature, ΔH_{A} is the reaction enthalpy (cal mol^{-1}) and the universal gas constant $R = 1.9872$ when expressed in the units of $\text{cal mol}^{-1} \text{K}^{-1}$.

Table 9 Equilibrium Reactions in aqueous phase chemistry mechanism.

Equilibrium Reaction	K_A at 298 K (M or M atm ⁻¹)	$-\Delta H_A/R$ (K)	
$H_2O \leftrightarrow H^+ + OH^-$	1.00×10^{-14}	-6710	K_w
$CO_2 + H_2O \leftrightarrow CO_2 \cdot (aq)$	3.40×10^{-2}	2441	H_{co2}
$CO_2 \cdot (aq) \leftrightarrow H^+ + HCO_3^-$	4.30×10^{-7}	-1000	k_{c1}
$HCO_3^- \leftrightarrow H^+ + CO_3^{2-}$	4.68×10^{-11}	-1760	k_{c2}
$SO_2 + H_2O \leftrightarrow SO_2 \cdot (aq)$	1.23×10^0	3020	H_{so2}
$SO_2 \cdot H_2O \leftrightarrow H^+ + HSO_3^-$	1.30×10^{-2}	1960	k_{s1}
$HSO_3^- \leftrightarrow H^+ + SO_3^{2-}$	6.60×10^{-8}	1500	k_{s2}
$H_2SO_4 (aq) \leftrightarrow H^+ + HSO_4^-$	1.00×10^3	0	k_{svi1}
$HSO_4^- \leftrightarrow H^+ + SO_4^{2-}$	1.02×10^{-2}	2720	k_{svi2}
$NH_3 (g) + H_2O \leftrightarrow NH_3 \cdot (aq)$	6.20×10^1	4111	H_{hno3}
$NH_3 \cdot (aq) \leftrightarrow OH^- + NH_4^+$	1.70×10^{-5}	-4353	k_{a1}
$H_2O_2 + H_2O \leftrightarrow H_2O_2 (aq)$	7.45×10^4	6621	H_{h2o2}
$O_3 + H_2O \leftrightarrow O_3 (aq)$	1.13×10^{-2}	2300	H_{o3}
$HNO_3 + H_2O \leftrightarrow HNO_3 (aq)$	2.10×10^5	0.	H_{hno3}
$HNO_3 (aq) \leftrightarrow H^+ + NO_3^-$	1.02×10^{-2}	2720	k_n

The aqueous phase partitioning of species which undergo dissociation following dissolution in the cloud water (CO_2 , SO_2 , NH_3 , and HNO_3) can be described by an equations similar to eqn (6.10) above. This is demonstrated in the case of nitric acid where the aqueous form [$HNO_3(aq)$] readily disassociates into NO_3^- the nitrate ion.

$$[\text{HNO}_3(\text{aq})] = \frac{H_{\text{HNO}_3} p_{\text{O}_3}^0}{1 + 10^6 \text{LRTH}_{\text{HNO}_3}^*} \quad (6.12a)$$

where $H_{\text{HNO}_3}^*$ is the effective Henry's law coefficient for nitric acid.

$$H_{\text{HNO}_3}^* = H_{\text{HNO}_3} \left(1 + k_n / [\text{H}^+]\right); \text{ where } k_n = \frac{[\text{NO}_3^-][\text{H}^+]}{[\text{HNO}_3(\text{aq})]} \quad (6.12b)$$

The system of equations described above is closed by invoking the requirement of electro-neutrality. This yields the following charge balance equation.

$$\text{H}^+ + \text{NH}_4^+ = \text{OH}^- + \text{HCO}_3^- + \text{HSO}_3^- + 2\text{SO}_3^{2-} + 2\text{SO}_4^{2-} + 2\text{CO}_3^{2-} + \text{HSO}_4^- + \text{NO}_3^- \quad (6.13)$$

Eqn (6.13) can be expressed as a function of the partial pressures of each gas, the related Henry's law and equilibria coefficients and $[\text{H}^+]$.

$$[\text{NH}_4^+] = (H_{\text{nh}_3} k_{a1} p_{\text{nh}_3} / K_w) [\text{H}^+] \quad (6.14a)$$

$$[\text{OH}^-] = (k_w / [\text{H}^+]) \quad (6.14b)$$

$$[\text{HCO}_3^-] = (H_{\text{co}_2} k_{c1} p_{\text{co}_2} / [\text{H}^+]) \quad (6.14c)$$

$$[\text{HSO}_3^-] = (H_{\text{so}_2} k_{s1} p_{\text{so}_2} / [\text{H}^+]) \quad (6.14d)$$

$$[\text{SO}_3^{2-}] = (H_{\text{so}_2} k_{s1} k_{s2} p_{\text{so}_2} / [\text{H}^+]^2) \quad (6.14e)$$

$$[\text{CO}_3^{2-}] = (H_{\text{co}_2} k_{c1} k_{c2} p_{\text{co}_2} / [\text{H}^+]^2) \quad (6.14f)$$

$$[\text{NO}_3^-] = (H_{\text{hno}_3} k_n p_{\text{hno}_3} / [\text{H}^+]) \quad (6.14g)$$

$$[\text{HSO}_4^-] = \left[\frac{[\text{H}^+][\text{S}(\text{VD})]}{([\text{H}^+] + K_{\text{svi}2})} \right] \quad (6.14h)$$

$$[\text{SO}_4^{2-}] = \left[\frac{k_{\text{sv}2}[\text{S}(\text{VI})]}{([\text{H}^+] + K_{\text{svi}2})} \right] \quad (6.14i)$$

Substituting the terms in eqn (6.14) into eqn (6.13) yields a quasi cubic in $[H^+]$ (quasi because of the $[H^+]$ terms in the denominators of [eqn 6.14(h, i)], which can then be solved to give a charge balanced system.

6.3.2 Method of solution

Equations (6.7b) and (6.8b) are integrated for a full internal time step ($2\Delta t$ - see section 2.1) using an Euler predictor-corrector scheme as shown in Figure 5. The scheme is self starting and derives an initial integration time step from the rate of change of $[S(VI)]$.

$$\Delta t_{aq} = \varepsilon \frac{[S(IV)]}{R_{O_3} + R_{H_2O_2}} \quad (6.15)$$

Here Δt_{aq} is the aqueous chemistry solver time step; R_{O_3} , $R_{H_2O_2}$ are the reaction rates for eqn's 6.7(a) and 6.8(a) as previously defined; and $\varepsilon = 0(1)$ is a scaling factor which has been derived from numerical experiment and is used to ensure that the first guess time step doesn't lead to a highly inaccurate initial solution of eqn's (6.7b) and (6.8b).

The predictor-corrector scheme consists of an explicit Euler predictor for the first guess and an implicit Euler corrector which is called up to five times.

Predictor.

$$S(VI)_{O_3}^{t+\Delta t_{aq}} = S(VI)_{O_3}^t + R_{O_3}^t \Delta t_{aq} \quad (6.16a)$$

$$S(VI)_{H_2O_2}^{t+\Delta t_{aq}} = S(VI)_{H_2O_2}^t + R_{H_2O_2}^t \Delta t_{aq} \quad (6.16b)$$

Corrector.

$$S(VI)_{O_3}^{t+\Delta t_{aq},n+1} = S(VI)_{O_3}^{t,n} + R_{O_3}^{t,n} \Delta t_{aq} \quad (6.17a)$$

$$S(VI)_{H_2O_2}^{t+\Delta t_{aq},n+1} = S(VI)_{H_2O_2}^{t,n} + R_{H_2O_2}^{t,n} \Delta t_{aq} \quad (6.17b)$$

Error checking and time step control is used to ensure convergence of the scheme. For example, if the solution converges within five iterations, Δt_{aq} is increased by a factor of 1.1 prior to the

next integration sequence. If the solution doesn't converge then Δt_{aq} is decreased by a factor of 0.7 and the integration is re-started.

Each invocation of the predictor or corrector operators requires an updated value of R_{O_3} and $R_{H_2O_2}$. The calculation methodology for these rates is shown in Figure 6 and involves the calculation of the current equilibrium state between the gas phase species and the dissolved aqueous phase species and the related ionic species for the cloud air/water system. The calculation involves taking a first guess $[H^+]$ (2.5×10^{-6} M), calculating Henry's law coefficients and equilibrium constants (Table 9), calculating the concentrations of ionic species (equation 8) and calculating the charge balance. Depending upon whether the charge balance is positive or negative, a bisection algorithm is used to generate an improved estimate of $[H^+]$ and the whole process is repeated until $[H^+]$ converges to a stable value and the charge balance is approximately zero.

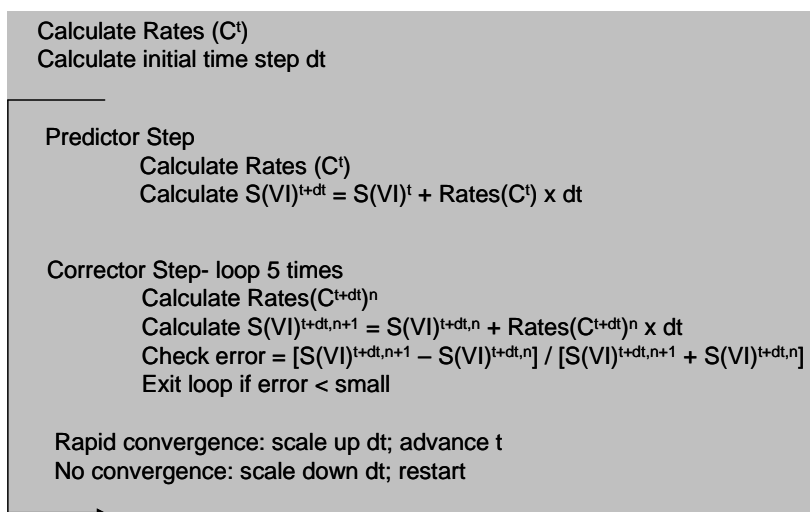


Figure 5 Schematic diagram showing how the predictor-corrector scheme is used to integrate eqn (6.7).

```

RATES

Bi-section search for CB (charge balance) = 0
Set initial [H+] bounds (CBlower × CBupper < 0)

Search loop
  [H+]mid = 0.5( [H+]lower + [H+]upper )
  Calculate Henry's law coefficients
  Calculate equilibrium reaction rates
  Calculate aqueous and ion concentrations
  Calculate partial pressures for gases
  Calculate CBmid

  Check error = ( [H+]mid - [H+]lower ) / ( [H+]mid - [H+]lower )
  Exit Search loop if error < small

  Check for CBlower × CBmid < 0 or CBupper × CBmid < 0
Search loop

Calculate S(IV) oxidation rates

```

Figure 6 Schematic diagram showing how a bi-section algorithm is used to solve for the charge balance shown in equation 7.

Integration of equations 6.7(b) and 6.8(b) for the full advection time step yields updated concentrations of sulphate in the cloud water and cloud rain. The fate of this dissolved S(VI) and the associated aqueous phase species then depends upon the cloud dynamics. For example S(VI) in cloud rain is advected towards the surface at the terminal velocity of the rain drops (see section 4.2.4). If the rain reaches the surface then the S(VI) mass is removed from the atmosphere and is added to the wet deposition mass. If the rain evaporates before hitting the surface then the S(VI) is added to non-aqueous particulate sulphate mass in the < 2.5 µm particle size category. S(VI) in the cloud water is treated similarly. Model cells which contain S(VI) but no cloud water are assumed to correspond to a region where the cloud water has either evaporated or rained out. Again the S(VI) mass is added to the non-aqueous particulate sulphate mass.

Table 10 lists the Carbon Bond 2005 species which must be present for the in-cloud sulphate model to operate. The unshaded rows correspond to the species present in the core Carbon Bond mechanism. The lightly shaded rows correspond to the species also required by the inorganic aerosol mechanism (section 6.1) and the heavily shaded rows correspond to the additional species required by the in-cloud sulphate mechanism. All of these species are present in the CB05_AER mechanism (Table 22).

EMISSIONS

Table 10 Core and extension Carbon Bond 2005 species required by cloud chemistry and secondary aerosol models.

Species CB05 name	Description	Molecular weight
O3	Ozone	48.0
SO2	Sulfur dioxide	64.1
H2O2	Hydrogen peroxide	36.0
HNO3	Nitric acid	63.0
NH3	Ammonia	17.0
NH4	Ammonium	18.0
ANIT	aerosol nitrate	62.0
ASO4	aerosol sulfate	96.1
WNIT	Nitric acid in cloud water/rain	63.0
WSO4	S(VI) in cloud water	96.1
RSO4	S(VI) in cloud rain	96.1

7. EMISSIONS

The CTM treats trace gas and aerosol emissions as time dependent volume sources. Emissions are defined in g s^{-1} for a respective grid point (in the curvilinear coordinates of the model) and are converted to $\text{molec cm}^{-3} \text{ s}^{-1}$ in the case of trace gas emissions and $\text{g m}^{-3} \text{ s}^{-1}$ in the case of aerosol emissions according to eqn (7.1).

$$E_i = \begin{cases} \frac{q_i N_a}{dx \cdot dy \cdot dz \cdot mw_i} \times 10^{-6} & \text{gas} \\ \frac{q_i}{dx \cdot dy \cdot dz} & \text{aerosol} \end{cases} \quad (7.1)$$

where q_i emission of species i from a given cell at a given time t ; N_a is Avogadro's number; dx , dy , dz are the cell dimensions and mw_i is the gram molecular weight of the i^{th} gaseous species.

7.1 Anthropogenic emissions

The CTM has online emissions algorithms which parameterise the temperature dependency of exhaust and evaporative emissions from motor vehicles, the plume rise of buoyant point sources. These algorithms are described in the next sections.

7.1.1 Motor vehicle emissions

Exhaust and evaporative emissions from motor vehicles are corrected for temperature within the CTM at each time step using predicted near surface temperatures. Temperature dependency is parameterised using bi-linear functions (Hurley 2008) which are prescribed as a function of vehicle fuel class (petrol, diesel, liquefied petroleum gas). The functions are shown in Figure 7. In the case of the tailpipe emissions it can be seen that the emissions of VOC and CO are minimised at 25°C and increase by 20–40% per 10°C. On the other hand, NO_x is modelled as a monotonic decreasing function of temperature. The temperature function for evaporative emissions temperature function is essentially a bi-linear representation of the exponential Reddy vapour generation equation (Reddy 1989) and can be seen to result in a factor of two variation of the evaporative emissions as the ambient temperature increases from 25 to 35 °C.

7.1.2 Elevated point source

The plume rise of sources emitted with vertical momentum or at above ambient temperatures is simulated using a simplified version of the numerical plume rise model used by TAPM and is described in detail in Hurley (2008).

7.2 Natural emissions

The CTM includes inline algorithms to model the emissions of VOC, NO_x and NH_3 from vegetation and soils, the emissions of sea salt aerosol, the emissions of wind blown dust, and the re-emission of elemental mercury emissions from soils, vegetation and water.

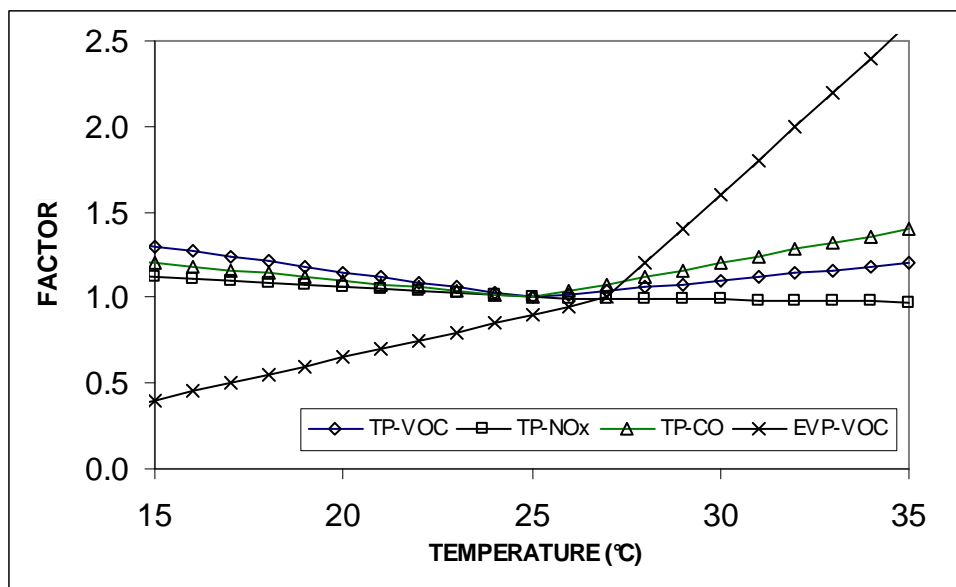


Figure 7 Ambient temperature correction functions for the tailpipe emissions of NO_x (TP-NO_x), VOC (TP-VOC) and CO (TP-CO); and evaporative emissions of VOC (EVP-VOC) from petrol-driven vehicles.

7.2.1 VOC emissions from forest canopies

The CTM includes an inline model of VOC emissions from forest canopies. The model divides the canopy into an arbitrary number of vertical layers (typically 10 layers are used). Layer-specific biogenic fluxes are generated using a normalised emission rate (normalised to 30°C and 1000 $\mu\text{mol m}^{-2} \text{s}^{-1}$) and descriptions of the in-canopy gradients of temperature, radiation and leaf mass. According to this approach, biogenic emissions from a forest canopy can be estimated from a prescription of the leaf area index LAI ($\text{m}^2 \text{m}^{-2}$), the canopy height h_c (m), the leaf biomass B_m (g m^{-2}), and a plant genera-specific leaf level VOC emission rate Q_{leaf} ($\mu\text{g-C g}^{-1} \text{h}^{-1}$) for the desired chemical species.

Considering the controlling variables further, we define LAI_t to quantify the total area of leaf (one-sided) per unit area of ground for a column extending from the ground to h_c . The leaf biomass B_m is the total dry weight of leaves extending from the ground to h_c per unit area of ground. The emission rate may be expressed in terms of carbon mass emitted per gram of dry biomass per hour ($\mu\text{g-C g}^{-1} \text{h}^{-1}$), or in units of $\mu\text{g-C m}^{-2} \text{h}^{-1}$, where area in this case refers to one-sided leaf area. Canopy-total emission rate may then be obtained by scaling the leaf-level emission rate by the LAI .

Leaf-level emission rate. The leaf-level emission rate is given by the following equation.

$$Q_{leaf} = q_{st} C_L C_T \quad (7.2)$$

Here q_{st} is a genera-specific, normalised emission rate (for a prescribed chemical species) and C_L , C_T are functions to correct q_{st} to alternative values of temperature and solar radiation flux. In the case of isoprene, the radiation function C_L is given by (Guenther et al., 1993):

$$C_L = \frac{\alpha \cdot c_{L1} \cdot L}{\sqrt{1 + \alpha^2 L^2}} \quad (7.3)$$

where $\alpha = 0.0027$, $C_{L1} = 1.066$ and L is the PAR flux ($\mu\text{mol m}^{-2} \text{s}^{-1}$).

The temperature function C_T is given by:

$$C_T = \frac{\exp\left(\frac{c_{T1}(T - T_S)}{RT_S T}\right)}{1 + \exp\left(\frac{c_{T2}(T - T_M)}{RT_S T}\right)} \quad (7.4)$$

where

$$R = 8.314 \text{ J K}^{-1} \text{ mol}^{-1}$$

$$C_{T1} = 95,000 \text{ J mol}^{-1}; C_{T2} = 230,000 \text{ J mol}^{-1}$$

$$T_M = 314 \text{ K}; T_S = 303 \text{ K is the standard temperature referred to above.}$$

Radiation function. It can be seen from eqn (7.2)-(7.4) that the leaf-level emissions require the specification of the leaf temperature and the incident radiation flux. The attenuation of radiation through the canopy is determined using a relationship developed by Zang et al. (2001).

$$PAR_{shade} = R_{diff} e^{(-0.65LAI(z)^{1.5})} + 0.07R_{dir} (1.1 - 0.1LAI(z)) e^{-\cos\theta} \quad (7.5),$$

where PAR_{shade} is the PAR flux on the shaded leaves, R_{diff} is the diffuse PAR radiation at the top of the canopy, R_{dir} is the direct PAR radiation at the top of the canopy, $LAI(z)$ is the height dependent, local leaf area index of the canopy and θ is the solar zenith angle.

The PAR flux incident on the sunlit leaves is given by (Norman, 1982).

$$PAR_{sun} = R_{dir} \cos \delta / \cos \theta + PAR_{shade} \quad (7.6).$$

where δ is the mean angle between the leaves and the sun.

Sunlit and shaded leaf area index. Following Norman (1982), the cumulative (integrated from h_c down) LAI of sunlit and shaded leaves is given by

$$LAI_{sun} = 2 \cos \theta [1 - e^{(-0.5LAI/\cos \theta)}] \quad (7.7)$$

$$LAI_{shade} = LAI - LAI_{sun} \quad (7.8)$$

Temperature function. During daylight hours, leaf level temperature is approximated by a LAI -weighted interpolation of the leaf temperature at the top of the canopy and the temperature at the canopy base.

$$T_{leaf}(z) = T_h + (LAI(z)/LAI_t)[T_{base} - T_h] \quad (7.9)$$

where T_h is the leaf temperature at h_c (defined below), and T_{base} is the under-canopy temperature. For a dense canopy, surface energy fluxes are small and thus (in the absence of horizontal temperature advection) temperatures at the base of the canopy will exhibit little diurnal variation. Thus we use a 24-hour average temperature (derived from the screen temperature) as an approximation of the under-canopy temperature.

During nocturnal conditions, a height-based linear interpolation replaces eqn (7.9). Note that the approach described above represents a simplification of the more rigorous approach of determining leaf-level temperature through solution of a surface-energy balance equation (i.e. Lamb et al. 1993). However, such a system is currently too computationally demanding for inclusion within the CTM.

Layer-specific emission rate. Following the prescription of the layer-specific leaf temperature, solar radiation flux and LAI , a leaf-level biogenic VOC emission rate for the i^{th} layer may be calculated using the following expression.

$$Q_{leaf}^i = q_{st} \bullet C_T^i [C_{Lsun}^i LAI_{sun}^i + C_{Lshade}^i LAI_{shade}^i] \quad (7.10)$$

It can be seen from (7.10) that the emission rate is a LAI -weighted sum of the flux from the sunlit and shaded areas of the leaf.

Canopy total emission rate. The canopy-cumulative emission rate ($\mu\text{g-C m}^{-2} \text{h}^{-1}$) is then given by (for an n -layer canopy),

$$Q_{\text{canopy}} = q_{st} \cdot B_m \sum_{i=1}^{n\text{-layer}} C_T^i [C_{Lsun}^i LAI_{sun}^i + C_{Lshade}^i LAI_{shade}^i] / LAI_t \quad (7.11)$$

The canopy model requires the prescription of direct and diffuse PAR at h_c , leaf temperature at h_c , total and vertical distribution of LAI, biomass and normalised leaf-level emission flux.

In the current system, clear sky radiation fluxes are determined according to the scheme of Weiss and Norman (1985).

Leaf temperature is approximated from Monin Obukhov similarity theory using the near-surface temperature (i.e. from the first level of a numerical model).

$$T_l = T_z \left\{ 1 - (u_* / k)^2 / gL [\log(z/z_h) - \Psi_H(z/L) + \Psi_H(z_h/L)] \right\} \quad (7.12)$$

Here u_* is the friction velocity, k is von Karman's constant, L is the Monin Obukhov length, z_h is the roughness height for heat (which we take as $0.1 z_0$; Hess 1992) and Ψ_H is the profile stability correction for heat.

In TAPM-CTM, the leaf area index and land use maps are taken from the data bases provided with TAPM (Hurley 2008). The normalised emission rates are currently based on Australian observations (i.e. Azzi et al. 2005) although these can be changed at model run time to suit the local vegetation characteristics. The vertical distribution of LAI is taken to follow a triangular distribution (Lamb et al. 1993), with the peak LAI occurring at two-thirds of the canopy height and LAI dropping to zero at one-third of canopy height.

7.2.2 VOC emissions from pasture and grasses

The pasture emission model is taken from Kirstine et al. (1998), who undertook numerous measurements of total and speciated VOC over pasture in a site in south eastern Victoria, Australia. The authors observed the total VOC emission rates to vary between zero and more than $1.5 \text{ mg-C m}^{-2} \text{h}^{-1}$. VOC emission rates were observed to have strong radiation and temperature dependencies. Emissions dropped to undetectable levels during night-time

conditions. In contrast to eucalypts VOC emissions, oxygenated species such as methanol, ethanol and acetone comprised the dominant VOC species emitted from pastures and grasses.

Kirstine et al. undertook a least-squares non-linear regression of their results, yielding the following equation for total VOC emission flux over grass.

$$Q_{grass} = 1.40819 \times 10^{-9} q_{st} B_m PAR^3 (2.46 \times 10^{-3} T_l^2 - 6.22 \times 10^{-7} T_l^4 - 1) \quad (7.13),$$

where $PAR = R_{diff} + R_{dir}$.

The clear sky radiation fluxes are determined according to the scheme of Weiss and Norman 1985, and leaf temperature is approximated by eqn (7.12).

Biomass totals and normalised emission rates are taken from Kirstine et al. (1998). In particular, they observed a mean, normalised emission rate of $0.4 \mu\text{g-C m}^{-2} \text{h}^{-1}$. Leaf biomass for pasture was observed to vary between a maximum of 2300 g m^{-2} (during the growing season), reducing to 940 g m^{-2} by the end of summer. This yielded a seasonal average biomass density of 1600 g m^{-2} . We have adopted a biomass density of 1000 g m^{-2} , given that an important application of the biogenic emissions system is to provide input into the modelling of photochemical smog events. Many photochemical smog events occur in mid- to late summer, after the growth season has ended.

Kirstine et al. (1998) analysed a number of the VOC samples for individual organic species. On the basis of their observations, the VOC carbon mass predicted by eqn (7.13) is speciated into methanol (13 %), ethanol (18 %), acetaldehyde (14 %), acetone (16 %), isoprene (5 %) and monoterpene (5 %).

7.2.3 Natural NO_x emissions

Natural emissions of oxides of nitrogen are modelled according to the approach given in Carnovale et al. (1996) and Williams et al. 1992. Natural NO_x emissions for Australian land use and soil conditions are taken from Galbally and Weeks (1992) and Duffy et al. (1988) and are listed in Table 11.

NO_x emissions from soil are observed to vary with soil temperature and are parameterised as follows (Williams et al. 1992).

$$Q_{nox} = Q_{nox}^s \exp[0.71(T - 30)] \quad (7.14)$$

where Q_{nox}^s is the NO_x emission rate at 30°C and T is the soil temperature (°C).

Table 11 NO_x and NH₃ emission rates from natural landscapes

Landscape	NO_x emission rate (ng-N m⁻² s⁻¹)	NH₃ emission rate (ng m⁻² s⁻¹)
Forest	0.38	1.2
Shrubland	1.0	1.3
Pastureland	2.88	0.9
Urban	0.29	n/a
Water	0.3	-
Desert	n/a	0.3

7.2.4 Natural NH₃ emissions

The ammonia emission model is based on a simple approach summarised in Battye and Barrows (2004). The approach uses annual average emission factors which are prescribed for four natural landscapes (Table 11). Seasonal and diurnal emission factors are also provided by the authors. In the current study, these landscape-dependant emission factors have been mapped to the 38 land use categories used by the CTM and applied without modification for season. A diurnal variation in the ammonia emissions has been included for the current study through the use of a top-hat function which restricts the emissions to daylight hours only.

Note that this approach is a highly simplified representation of the actual NH₃ emissions process. As discussed in Battye and Barrows, the sign and magnitude of the natural NH₃ flux is determined by whether the vegetation is emitting or absorbing ammonia, with the direction of the NH₃ flux controlled by the NH₄⁺ ion concentrations in the leaves and the NH₃ gaseous

concentrations within the vegetation canopy. Over short periods of time (i.e. diurnal time scales), the net NH_3 flux has been observed to vary over two orders of magnitude. As such it is clear that a considerable degree of uncertainty is associated with the application of the emission rates as listed in Table 11.

7.2.5 Sea salt emissions

Sea salt aerosol is produced by breaking waves, with the dominant mechanism being film and jet drops generated by the bursting of entrained air bubbles (Gong et al. 1997). The CTM uses the algorithm of Monahan et al. (1986) and the modification of Gong (2003) to model sea salt aerosol emissions from the open ocean.

$$\frac{dF_0}{dr} = 1.373u_{10}^{3.41}r^{-a}(1 + 0.057r^{3.45}) \times 10^{1.607e^{-B^2}} \quad (7.15)$$

where F_0 is the rate of droplet generation per unit area per increment of particle radius ($\text{m}^{-2} \text{s}^{-1} \mu\text{m}^{-1}$), u_{10} is the wind speed at 10 metre height, r is the particle radius (at a relative humidity of 80%); and the constants

$$a = 4.7(1 + 30r)^{-0.017r^{-1.44}} \quad \text{and} \quad b = (0.433 - \log_{10}(r))/0.433$$

Sea salt emissions in the range 0.1 – 2.5 μm and 2.5 – 10 μm may be generated and transported in the CB05_AER version of the Carbon Bond 2005 mechanism (see Table 22).

7.2.6 Wind blown dust emissions

Wind blown dust emissions are modelled using the Lu and Shao (1999, 2001) approach. The approach is based on three concepts. 1- a threshold friction velocity above which the surface shear stress is sufficient to overcome cohesive forces and to mobilise soil particles; 2- a horizontal flux of saltating sand particles, where saltation refers to a bouncing movement of particles over a land surface along the mean direction of the wind, and sand particles refers to the fraction of the mobilised soil particles which are too large to become suspended in the atmosphere by turbulence; 3- a vertical flux of dust (the particle fraction which is small enough to become suspended), generated from soil particles displaced by cratering impacts of the saltating particles.

Threshold Friction Velocity

The threshold friction velocity u_{*f} is the minimum friction velocity required to initialise particle movement. u_{*f} is a function of particle size, particle density, surface roughness elements, soil moisture and soil aggregation and crusting. Lu and Shao (2001) present the following parameterisation of u_{*f} .

$$U_{*f}(d) = u_{*f0}(d)RHM \quad (7.16)$$

$$u_{*f0} = \sqrt{a_1(\sigma_p g d + \frac{a_2}{\rho d})} \quad (7.17)$$

Here u_{*f0} is the threshold friction velocity for a bare, dry and loose soil surface. u_{*f0} is a function of particle diameter d , density ρ , and the acceleration due to gravity g . σ_p is the particle-to-air density ratio. $a_1=0.0123$ and $a_2=3 \times 10^{-4} \text{ kg s}^{-2}$. R corrects u_{*f0} for the effect of non-erodible surface roughness elements, H corrects u_{*f0} for the effects of soil moisture and M corrects u_{*f0} for the effects of soil surface aggregation and crusting. Expressions for R and H are empirically determined and the function M is currently set to 1 for all soil types. See Shao *et al.* (1996) for further details regarding these parameters.

Particle Terminal Velocity

Soil particles that can be readily suspended in the atmosphere are defined as dust. The propensity for suspension is determined by the ratio of the particle terminal velocity w_t and the mean Lagrangian turbulent vertical velocity scale. Following Lu and Shao (2001) the upper size limit for dust particles follows from the solution of (7.16).

$$w_t(d) = 0.7 u_{*f} \quad (7.18)$$

where $w_t(d)$ is the terminal velocity for particles with diameter d . For example, $u_{*f} = 0.8 \text{ m s}^{-1}$ gives $d = 100 \text{ }\mu\text{m}$.

Horizontal Sand Flux

For a uniform soil, and for the condition $u_{*t}(d) < u_* < w_t(d)$, the horizontal sand flux is calculated as follows (Owen 1964).

$$\tilde{Q} = (c\rho u_*^3 / g)[1 - (u_{*t}(d)/u_*)^2] \quad (7.19)$$

Here c is Owen's coefficient. In practise, the total horizontal sediment flux, Q , is calculated as a weighted integral of \tilde{Q} over each size class of a representative particle size distribution (PSD) $p(d)$. Here we use 25 dust particle classes in the range 2–125 μm (with the upper bound determined dynamically using [7.16]). The soil PSD has 38 classes in the range 2–1159 μm . Upper bounds from 90 to 125 μm (medium sand) were included to account for severe wind erosion events.

$$Q = \int \tilde{Q}(d)p(d)\delta d \quad (7.20)$$

The effects of surface non-erodible elements, such as vegetation cover and the presence of rocks, are compensated for using E_s , a correction factor for presence of rocks and pebbles (see Table 2, Lu and Shao 2001) and E_v , a correction for vegetation cover calculated from leaf area index.

Vertical Dust Flux

The vertical dust flux, F resulting from each saltating particle-size category is related to the horizontal saltation flux, Q as follows

$$F = \frac{0.12C_\alpha g f \rho_b}{p} Q \quad (7.21),$$

where f is the total volumetric fraction of dust in the sediment (derived from the soil PSD), C_α is a coefficient of order 1, ρ_b is soil bulk density and p is the horizontal component of plastic flow pressure. The latter three terms are given in Table 2 of Lu and Shao (2001). The PSD used by the CTM is representative of a minimally dispersed soil size distribution, which assumes that soil aggregates and grains coated with dust are not broken into smaller size fractions as a result of the sand bombardment. By contrast the fully dispersed particle-size distribution

(FDPSD) accounts for the break-up of the soil aggregates and dust coatings. If the FDPSD is available, it can be used to provide information about the upper limits of dust emission. A later version of Shao's (2002) model accounts for the disintegration of dust coatings on sand grains and soil aggregates during saltation, a procedure that can significantly alter the PSD during a strong wind erosion event.

7.2.7 Mercury emissions

The CTM models the re-emissions of elemental mercury using the outlined in Shetty (2008) and references therein. Emissions from vegetation are assumed to be caused by the uptake of mercury in the soil-water via the porous plant root system. The plant vascular system then transports the mercury into the canopy atmosphere within water vapour released via stomata in the leaves (evapotranspiration). The resistance to vapour transport through the stomata varies with radiation, temperature, ambient water mixing ratio and soil water availability. For example plant stomata are only open when the leaves are exposed to solar radiation and moreover will close to regulate water vapour losses if the soil becomes dry or if leaf temperatures are too high. Because of the high temporal variability of stomata behaviour, mercury emissions from evapotranspiration are calculated on any hourly basis using stomatal resistances derived from the weather model outputs. Emissions are scaled up from leaf-level to grid scale using gridded fields of leaf area index (surface leaf area per m² of ground) and land cover.

The fluxes of mercury from soils are divided into two categories- mercury emitted from shaded soil (located under a canopy) and mercury emitted from a bare soil surface (Gbor et al. 2006). For bare soil, emissions are parameterised using the soil temperature and the soil mercury concentration while the emissions from shaded soils are expressed as a function of the under-canopy solar radiation flux and the soil mercury concentration. Shaded and bare soil mercury emissions are calculated on an hourly basis using soil temperatures and radiation fluxes taken from the weather model. The soil water mercury concentrations required for the vegetation mercury emission modelling are derived from soil mercury concentrations using a partitioning coefficient of 0.2 g L⁻¹ (Lyon et al. 1997).

Emissions from a water surface also use an approach described by Shetty et al. (2008). Here the mass transfer rate is driven by the difference between the equilibrium dissolved mercury concentration (derived from the modelled near-surface atmospheric mercury concentration using a Henry's law approach) and the ambient dissolved mercury concentration. In the absence

EMISSIONS

of dissolved mercury concentration observations for Australian coastal waters, we have used a mean aqueous concentration of 0.04 ng l^{-1} given in Xu et al. (1999).

REFERENCES

- Ansari A.s., Pandis S.N., 1999. Prediction of multi-component inorganic atmospheric aerosol behavior. *Atmos. Environ.*, 33, 745-757.
- Azzi M., Johnson G.J. and Cope M., 1992. An introduction to the Generic Reaction Set Photochemical smog mechanism. *Proc. 11th International Clean Air Conf.*, Brisbane, 5-10 July, 451-462.
- Azzi, M., et al., 2005. A biogenic volatile organic compounds emission inventory for the Metropolitan Air Quality Study (MAQS) region of NSW. In: Towards a new agenda: 17th International Clean Air & Environment Conference proceedings, Hobart. Clean Air Society of Australia and New Zealand. 7 p.
- Battye W. and Barrows R., 2004. Review of ammonia emission modelling techniques for natural landscapes and fertilized soils. EPA Contract No. 68-D-02-064. EC/R Incorporated Chapel Hill, NC 27517. 35pp.
- Byun D.W., 1999. Dynamically consistent formulations in meteorological air quality models for multiscale atmospheric studies. Part II: Mass conservations issues. *Journal of the Atmospheric Sciences* 56, 3808-3820.
- Carnovale F., Tilly K., Stuart A., Carvalho C., Summers M. and Eriksen P., 1996. Metropolitan air quality study: Air emissions inventory. *Final report to New South Wales Environment Protection Authority, Sydney Australia.*
- Cope M. E., Hess G. D., Lee S., Tory K., Azzi M., Carras J., Lilley W., Manins P. C., Nelson P., Ng L., Puri K., Wong N., Walsh S., Young M., 2004. The Australian Air Quality Forecasting System. Part I: Project Description and Early Outcomes. *J. Appl. Meteorol.*, 43, 649-662.
- Cope, M.E., Lee, s.H., Physick, W.L., Abbs D., McGregor, J.L, Nguyen, K.C., 2009. A Methodology for Determining the Impact of Climate Change on Ozone Levels in an Urban Area. Clean Air Research Project 11. Final report to Department of Environment, Water, Heritage and the Arts (DEWHA).
- Duffy L., Galbally I.E., and Elsworth M., 1988. Biogenic NO_x emissions in the Latrobe Valley. *Clean Air*, 22, 196-198. Clean air Society of Australia and New Zealand.
- Draxler R.R. and Hess G.D., 1997. Description of the HYSPLIT_4 modeling system. NOAA Technical Memorandum ERL ARL-224. Air Resources Laboratory Silver Spring, Maryland.
- EPA, 1999. Science Algorithms of the EPA Models-3 Community Multiscale Air Quality (CMAQ) Modeling System. EPA/600/R-99/030. Office of Research and Development. Washington DC 20460.
- Gbor, P.K, Wen, D., Meng, F., Yang, F., Zhang, B. and Sloan, J.J. ,(2006. Improved model for mercury emission, transport and deposition, *Atmos. Environ*, 40,973-983.

REFERENCES

- Galbally I.E. and weeks I.A., 1992. Natural emissions of hydrocarbons, nitrogen oxides, carbon monoxide and sulphur gases in the Kooragang Island region of Newcastle NSW. CSIRO Atmospheric Research, Aspendale, Victoria.
- Gong S.L, Barrie L.A and Blanchet J.P., 1997. Modeling sea-salt aerosols in the atmosphere 1. Model development. *Journal Geophys. Res.* 102, D3 pp 3805-3818.
- Gong S.L., 2003. A parameterisation of sea-salt aerosol source function for sub- and super-micron particles. *Global Biogeochemical Cycles*, V 17, 4, 1097, doi:10.1029/2003GB002079
- Guenther A., Zimmerman P., Harley P., Monson R. and Fall R., 1993. Isoprene and monoterpene emission rate variability: model evaluation and sensitivity analysis. *J. Geophys. Res.*, **98D**, 12,609-12,617.
- Hess G.D., 1989. A photochemical model for air quality assessment: model description and verification. *Atmos. Environ.*, 23, 643-660.
- Hess G.D., 1992. Observations and scaling of the atmospheric boundary layer. *Aust. Met. Mag.* **41**, 79-99.
- Hoffmann, M.R., and Calvert, J.G., 1985. Chemical Transformation Modules for Eulerian Acid Deposition Models, Volume 2, The Aqueous-Phase Chemistry, EPA/600/3-85/017. U.S. Environmental Protection Agency, Research Triangle Park, NC.
- Hu Y., Odman M.T., 2008. A comparison of mass conservation methods for air quality models. *Atmos. Environ.* 42, 8322-8330.
- Hurley P., 2008. TAPM v4. Part 1: Technical Description. CSIRO Marine and Atmospheric Research. ISBN: 978-1-921424-71-7. ISSN: 1835-1476.
- Keywood M., and Cope M.E., 2009. Development of Tools for the Identification of Secondary Organic Aerosol in Australian Cities. Clean Air Research Project 15. Final report to Department of Environment, Water, Heritage and the Arts.
- Kirstine W., Galbally I.E, Ye Y., and Hooper M.A., 1998. Emissions of volatile organic compounds (primary oxygenated species) from pasture. *J. Geophys. Res.*, 103, 100605-10620.
- Kitada T., 1987. Effect of non-zero divergence wind fields on atmospheric transport calculations. *Atmos. Environ.*, 21, 785-788.
- Lamb B., Gay D. and Westberg H., 1993. A biogenic hydrocarbon emission inventory for the U.S.A using a simple forest canopy model. *Atmos. Environ.*, 27A 1673-1690.
- Lyon, B.f., Ambrose, R., Rice, G., Maxwell, C.J., 1997. Calculation of soil–water and benthic sediment partition coefficients for mercury. *Chemosphere* 35, 791–808.
- Lu H. and Shao Y. 1999, ‘A new model for dust emission by saltation bombardment’, *J. Geophys. Res.*, 104:16827-42.
- Lu H. and Shao Y. 2001, ‘Toward quantitative prediction of dust storms: an integrated wind erosion modelling system and its applications’, *Env. Modelling & Software*, 16:233-49.

- Lurmann F.W., Carter W.P. and Coyner L.A., 1987. A surrogate species chemical reaction mechanism for urban scale air quality simulation models. *Final report to U.S. Environment Protection Agency under Contract Number 68-02-4104*.
- Marchuk G.I., 1974. Numerical methods in weather prediction. *Academic Press, New York*.
- Mathur, R., Young, J.O., Cshere, K.L. and Gipson G/L. (1998). A comparison of numerical techniques for solution of atmospheric kinetic equations. *Atmospheric Environment*, **32**, 1535-1553.
- McGregor, J. L., 2005. CCAM: Geometric aspects and dynamical formulation. CSIRO Atmospheric Research Tech. Paper No. 70, 43 pp.
- McRae G.J., Goodin W.R. and Seinfeld J.H., 1982. Mathematical Modelling of Photochemical Pollution. *EQL Report No. 18, 661 pp. (Environmental Quality Laboratory, California Institute of Technology: Pasadena)*.
- Monahan E.C., Spiel D.E. and Davidson K.L., 1986. A model of marine aerosol generation via whitecaps and wave disruption. In *Oceanic Whitecaps*, edited by E. C. Monahan and G. Mac Niocaill 167-174. D. Reidel, Norwell, Mass. U.S.A.
- Morris, R. et al., 2006. Model sensitivity for organic using two multi-pollutant air quality models that stimulate regional haze in the southeastern United States. *Atmospheric Environment*, **40**, 4960-4972.
- Nenes A., Pandis S.N., Pilinis C., 1998. ISORROPIA: A new thermodynamic equilibrium model for multiphase multi-component inorganic aerosols, *Aquat. Geoch.*, **4**, 123-152.
- Norman J.M., 1982. Simulation of microclimates. In: Hatfield, J.L., Thomason, I.J. (Eds.), *Biometeorology in Integrated Pest Management*. Academic Press, New York, 65-99.
- Odman M.T., Russell, A.G., 2000. Mass conservative coupling of non-hydrostatic meteorological models with air quality models. In: Gryning, S.-E., Batchvarova, E. (Eds.), *Air Pollution Modeling and Its Application Xiii*. Kluwer Academic/Plenum Publishers, New York, pp. 651-660.
- Odum, J.R., et al., 1996. 'Gas/particle partitioning and secondary organic aerosol formation. *Environmental Science and Technology*, **30**(8): 2580-2585.
- Pankow, J. F., 1994. An absorption model of gas-particle partitioning involved in the formation of secondary organic aerosol. *Atmospheric Environment* **28A**, 189-193.
- Pun, B., Seigneur, C., and Lohman, K., 2006. Modelling secondary organic aerosol formation from multiphase partitioning with molecular data. *Environmental Science and Technol.*, **40**, 4722-2731
- Pun B.K., and Seigneur C., 2007. Investigative modelling of new pathways for secondary organic aerosol formation. *Atmos. Chem. Phys.*, **7**, 2199-2216.

REFERENCES

- Puri, K., Dietachmayer, G., Mills, G.A., Davidson, N.E., Bowen, R.A., Logan, L.W., 1998. The new BMRC Limited Area Prediction System, LAPS. *Australian Meteorological Magazine*, 47, 203-233.
- Reddy, S.R., 1989. Prediction of fuel vapour generation from a vehicle fuel tank as a function of fuel RVP and Temperature. SAE 892099.
- Singh L., Cope M., and Azzi M., 2007. Modelling the contribution of secondary organic aerosol in air pollution events – from smog chamber to airshed. 14th IUAPPA World Congress Clean air partnerships: coming together for clean air : Brisbane 2007 : conference proceedings, incorporating the 18th CASANZ Conference hosted by the Clean Air Society of Australia and New Zealand, Brisbane Convention and Exhibition Centre. Brisbane: IUAPPA; CASANZ. 7 p.
- Saxena P., Hudischewskyj A., Seigneur C., and Seinfeld J., 1986. A comparative study of equilibrium approaches to the chemical characterization of secondary aerosols. *Atmos. Environ.*, 7, 1471-1483.
- Seinfeld J., and Pandis S., 1998. Atmospheric chemistry and physics. From air pollution to climate change. Wiley-Interscience. ISBN 0-471-17815-2.
- Shao Y., Raupach M. R. & Leys J. 1996, 'A model for predicting Aeolian sand drift and dust entrainment on scales from paddock to region', *Aust. J. Soil Res.,ceedings*, 34:309-42.
- Shao Y. 2002, 'A model for mineral dust emission', *J. Geophys. Res.*, **106**:20239-54.
- Shetty, S., Lin,C.,Streets, D. and Jang, C., 2008. Model estimate of mercury emission from natural sources in East Asia, *Atmos. Environ*, 42, 8674-8685.
- Smagorinsky J., 1963. General circulation experiments with the primitive equations 1. The basic experiment. *Mon. Weath. Rev.* 91, 99-164.
- Takakawa, H., et al., 2003. Temperature dependence of secondary organic aerosol formation by photo-oxidation of hydrocarbons. *Atmospheric Environment* 37 3413-3424.
- Toon O.B., Turco R.P., Westphal D., Malone R. and Liu M.S., 1998. A multidimensional model for aerosols: description of computational analogs. *Journal of Atmospheric Sciences* 45 (15) 2123-2143.
- Weiss A. and Norman J.M., 1985. Partitioning solar radiation into direct and diffuse visible and near-infrared components. *Agricultural and Forest Meteorology*. **34**, 205-213.
- Wesely, M.L., 1989. Parameterisation of surface resistances to gaseous dry deposition in regional-scale numerical models. *Atmos. Environ.*, **23**, 1293-1304.
- Williams E., Guenther A., and Fehsenfeld F., 1992. An inventory of nitric oxide emissions from soils in the United States. *J Geophys. Res.*, 97, D7 7511-7519.
- Yamartino R.J., 1993. Nonnegative conserved scalar transport using grid-cell-centred, spectrally constrained Blackman cubics for applications on a variable-thickness mesh. *Mon. Wea. Rev.*, **121**, 753-763.

Yarwood G., Rao S., Yocke M., Whitten G., 2005. Updates to the Carbon Bond chemical mechanism.: CB05. Final report RT-04-00675 to U.S. Environmental Protection Agency, Research Triangle Park, NC 27703.

Zhang L., Moran M., and Brook J.R., 2001. A comparison of models to estimate in-canopy photosynthetically active radiation and their influence on canopy stomatal resistance. *Atmos. Environ.*, 35, 4463-4470.

Xu, X., Yang, X., Miller, D., Helble, J., Carley, R., 1999. Formulation of bi-directional atmospheric–surface exchanges of elemental mercury. *Atmos. Environ.* 33 (27),1 4345–4355.

APPENDIX A –CHEMICAL TRANSFORMATION MECHANISMS

The following tables documents the chemical mechanisms currently supported by the CTM. The reaction rate types and coefficients are described in Table 2 and, and a summary of each mechanism is given in Table 4 of the main report.

In the species listings given below, de/ss refers to whether a species is transported and tendencies treated by the chemical mechanism differential equation solver- or treated as steady-state and solved by analytic or a mixed analytic/iterative solver; g/a refers to whether a species is a gas or an aerosol.

1. NOX mechanism

Mechanism name: NOX

Reference

N/A

Table 12 NOX mechanism

Short Name	Long Name	de/ss	g/a	mw (g)
NO	'nitric oxide'	DE	g	30
NO2	'nitrogen dioxide'	DE	g	46

The NOX mechanism has no chemical reactions.

2. OX mechanism

Mechanism name: OX

Reference

N/A

Table 13 OX mechanism species listing

Short Name	Long Name	de/ss	g/a	mw (g)
NO	'nitric oxide'	DE	g	30
NO2	'nitrogen dioxide'	DE	g	46
O3	'ozone'	DE	g	48
O	'oxygen singlet P'	SS	g	1

Table 14 OX mechanism reactions

REACTION	RATE	VARIABLE						
NO2 => NO + O	PHOT	1	1					
O + O2 + M => O3 + M	TDCN	6.00E-34	-2.4					
O3 + NO => NO2	ARRH	3.00E-12	1500					

3. Generic Reaction Set Mechanism

Mechanism name: GRS

Reference

Azzi M., Johnson G.J. and Cope M., 1992. An introduction to the Generic Reaction Set Photochemical smog mechanism. *Proc. 11th International Clean Air Conf.*, Brisbane, 5-10 July, 451-462.

Table 15 GRS mechanism species listing

Short Name	Long Name	de/ss	g/a	mw (g)
NO	'nitric oxide'	DE	g	30
NO2	'nitrogen dioxide'	DE	g	46
ROC	'reactive organic carbon'	DE	g	13.7
RP	'radical product'	SS	g	33
O3	'ozone'	DE	g	48
SGN	'stable gaseous nitrate'	DE	g	63
SNGN	'stable non-gaseous nitrate'	DE	g	63

Table 16 GRS mechanism

REACTION	RATE	VARIABLE						
ROC => ROC + RP	GRS1	1	-4700	0.00316				
NO + RP => NO2	CONS	8.13E-12						
NO2 => NO + O3	PHOT	1	1					
NO + O3 => NO2	ARRH	2.10E-12	1450					
RP + RP => RP	CONS	6.76E-12			-0.7	0.6		
NO2 + RP => SGN	CONS	8.12E-14			0	0.6		
NO2 + RP => SNGN	CONS	8.12E-14						

4. Mercury mechanism

Mechanism name: HG3T

Reference

N/A

Table 17 HG3T species listing

Short Name	Long Name	de/ss	g/a	mw (g)
hg0	'elemental mercury'	DE	g	200
rgm	'reactive gas mercury'	DE	g	271.5
hgp	'mercury aerosol'	DE	a	1

The HG3T mechanism has no chemical reactions.

5. Lurmann, Carter, Coyner mechanism

Mechanism name: LCC

Reference

Lurmann F.W., Carter W.P. and Coyner L.A., 1987. A surrogate species chemical reaction mechanism for urban scale air quality simulation models. *Final report to U.S. Environment Protection Agency under Contract Number 68-02-4104.*

Table 18 LCC species listing.

Short Name	Long Name	de/ss	g/a	mw (g)
NO	'nitric oxide'	DE	g	30
NO2	'nitrogen dioxide'	DE	g	46
O3	'ozone'	DE	g	48
HONO	'nitrous acid'	DE	g	47
HNO3	'nitric acid'	DE	g	63
HNO4	'pernitric acid'	DE	g	79
N2O5	'nitrogen pentoxide'	DE	g	108
NO3	'nitrate radical'	DE	g	62
HO2	'hydroperoxy radical'	DE	g	33
H2O2	'hydrogen peroxide'	DE	g	36
CO	'carbon monoxide'	DE	g	28
CO_B	'carbon monoxide bc tracer'	DE	g	28
CO_E	'carbon monoxide bc+e tracer'	DE	g	28
HCHO	'formaldehyde'	DE	g	30
ALD2	'lumped aldehyde'	DE	g	46
MEK	'methyl ethyl ketone'	DE	g	72.1
MGLY	'methylglyoxyl'	DE	g	72

APPENDIX A –CHEMICAL TRANSFORMATION MECHANISMS

PAN	'peroxyl acyl nitrate'	DE	g	121
RO2	'total RO2 radicals'	DE	g	1
MCO3	'CH3CO3 radical'	DE	g	1
ALKN	'alkyl nitrate'	DE	g	1
ALKA	'->C3 alkanes'	DE	g	81.2
ETHE	'ethene'	DE	g	28
ALKE	'->C2 alkenes'	DE	g	46.7
TOLU	'toluene'	DE	g	92
AROM	'aromatics'	DE	g	111.2
DIAL	'unknown dicarbonyls'	DE	g	1
CRES	'cresole'	DE	g	108.1
NPHE	'nitrophenols'	DE	g	1
MEOH	'methanol'	DE	g	32
ETOH	'ethanol'	DE	g	46
MTBE	'methyl tert-butyl ether'	DE	g	88
SO2	'sulfur dioxide'	DE	g	64.1
SO3	'sulfuric acid'	DE	g	98.1
ISOP	'isoprene'	DE	g	68.1
CH4	'methane'	DE	g	16
O1D	'oxygen singlet D'	SS	g	1
O	'o atom'	SS	g	1
OH	'hydroxy radical'	SS	g	1
RO2R	'general RO2 #1'	SS	g	1
R2O2	'general RO2 #2'	SS	g	1
RO2N	'alkyl nitrate RO2'	SS	g	1
RO2P	'phenol RO2'	SS	g	1
BZN2	'benzaldehyde N-RO2'	SS	g	1
BZO	'phenoxy radical'	SS	g	1
PM25	'PM25 inert species'	DE	a	1

APPENDIX A –CHEMICAL TRANSFORMATION MECHANISMS

Table 19. LCC mechanism.

REACTION	RATE	VARIABLE					
NO2 => NO + O	PHOT	1	1				
O => O3	ARRH	1.05E+03	-1282				
O + NO2 => NO	CONS	9.28E-12					
O + NO2 => NO3	ARRH	1.11E-13	-894				
NO + O3 => NO2	ARRH	1.80E-12	1370				
NO2+ O3 => NO3	ARRH	1.20E-13	2450				
NO + NO3 => 2.0*NO2	ARRH	7.99E-12	-252				
NO + NO => 2.0*NO2	ARRH	1.64E-20	-529				
NO2 + NO3 => N2O5	ARRH	4.62E-13	-273				
N2O5 => NO2 + NO3	ARRH	1.33E+15	11379				
N2O5 + H2O => 2.0*HNO3	CONS	1.00E-21					
NO2 + NO3 => NO + NO2	ARRH	2.50E-14	1229				
NO3 => NO	PHOT	8	1				
NO3 => NO2 + O	PHOT	1	33.9				
O3 => O	PHOT	1	0.053				
O3 => O1D	PHOT	2	1				
O1D + H2O => 2.0*OH	CONS	2.20E-10					
O1D => O	CONS	7.20E+08					

NO + OH => HONO	ARRH	4.04E-13	-833					
HONO => NO + OH	PHOT	1	0.197					
2.0*NO2 + H2O => HONO +1.0*HNO3	CONS	4.00E-24						
NO2 + OH => HNO3	ARRH	9.58E-13	-737					
HNO3 + OH => NO3	ARRH	9.40E-15	-778					
CO + OH => HO2	CONS	2.18E-13						
O3 + OH => HO2	ARRH	1.60E-12	942					
NO + HO2 => NO2 + OH	ARRH	3.70E-12	-240					
NO2 + HO2 => HNO4	ARRH	1.02E-13	-773					
HNO4 => NO2 + HO2	ARRH	4.35E+13	10103					
HNO4 + OH => NO2	CONS	4.00E-12						
O3 + HO2 => OH	ARRH	1.40E-14	579					
HO2 + HO2 => H2O2	ARRH	2.27E-13	-771					
HO2 + HO2 + H2O => H2O2	ARRH	3.26E-34	-2971					
NO3 + HO2 => HNO3	ARRH	2.27E-13	-771					
NO3 + HO2 + H2O => HNO3	ARRH	3.26E-34	-2971					
RO2 + NO => NO	ARRH	4.20E-12	-180					
RO2 + HO2 => HO2	CONS	3.00E-12						
RO2 + RO2 => NR	CONS	1.00E-15						
RO2 + MCO3 => NR	CONS	3.00E-12						
HCHO => 2.0*HO2 + CO	PHOT	3	1					

APPENDIX A –CHEMICAL TRANSFORMATION MECHANISMS

HCHO => CO	PHOT	4	1					
HCHO + OH => HO2 + CO	CONS	8.92E-12						
HCHO + NO3 => HNO3 + HO2 + CO	ARRH	5.99E-13	2060					
HCHO + HO2 => RO2R + RO2	CONS	1.00E-14						
ALD2 + OH => MCO3	ARRH	6.90E-12	-250					
ALD2 => CO + HCHO + RO2R + HO2 + RO2	PHOT	5	1					
ALD2 + NO3 => HNO3 + MCO3	ARRH	3.00E-13	1427					
MCO3 + NO => NO2 + HCHO + RO2R + RO2	ARRH	4.20E-12	-180					
MCO3 + NO2 => PAN	ARRH	2.79E-12	-180					
MCO3 + HO2 => HCHO	CONS	3.00E-12						
MCO3 + MCO3 => 2.0*HO2 + 2.0*HCHO	CONS	2.50E-12						
PAN => MCO3 + NO2	ARRH	2.00E+16	13542					
MEK => MCO3 + ALD2 + RO2R + RO2	PHOT	7	1					
MEK + OH => 1.2*R2O2 + 1.2*RO2 + MCO3 + 0.5*ALD2 + 0.5*HCHO	ARRH	1.20E-11	745					
MGLY => MCO3 + HO2 + CO	PHOT	3	6					
MGLY + OH => MCO3 + CO	CONS	1.70E-11						
MGLY + NO3 => HNO3 + MCO3 + CO	ARRH	3.00E-13	1427					
ALKA + OH => 0.1236*HCHO + 0.4021*ALD2 + 0.6155*MEK + 0.1191*RO2N + 0.8809*RO2R + 0.6928*R2O2 + 1.5737*RO2	ARRW	0.6057	1.05E-11	354	0.3943	1.62E-11	289	
ALKN + OH => NO2 + 0.15*MEK + 1.53*ALD2 + 0.16*HCHO + 1.39*R2O2 + 1.39*RO2	ARRH	2.19E-11	709					
RO2N + NO => ALKN	ARRH	4.20E-12	-180					

APPENDIX A –CHEMICAL TRANSFORMATION MECHANISMS

RO2N + HO2 => MEK	CONS	3.00E-12						
RO2N + RO2 => RO2 + 0.5*HO2 + MEK	CONS	1.00E-15						
RO2N + MCO3 => HCHO + HO2 + MEK	CONS	3.00E-12						
R2O2 + NO => NO2	ARRH	4.20E-12	-180					
R2O2 + HO2 => NR	CONS	3.00E-12						
R2O2 + RO2 => RO2	CONS	1.00E-15						
R2O2 + MCO3 => HCHO + HO2	CONS	3.00E-12						
RO2R + NO => NO2 + HO2	ARRH	4.20E-12	-180					
RO2R + HO2 => NR	CONS	3.00E-12						
RO2R + RO2 => 0.5*HO2 + RO2	CONS	1.00E-15						
RO2R + MCO3 => HO2 + HCHO	CONS	3.00E-12						
ETHE + OH => RO2R + RO2 + 1.56*HCHO + 0.22*ALD2	ARRH	2.15E-12	-411					
ETHE + O3 => HCHO + 0.12*HO2 + 0.42*CO	ARRH	1.20E-14	2634					
ETHE + O => RO2R + RO2 + CO + HCHO + HO2	ARRH	1.04E-11	792					
ETHE + NO3 => RO2 + NO2 + 2.0*HCHO + R2O2	ARRH	2.00E-12	2925					
ALKE + OH => RO2 + RO2R + 0.6640*HCHO + 1.3360*ALD2	ARRW	0.664	4.85E-12	-504	0.336	1.10E-11	-549	
ALKE + O3 => 0.4250*HCHO + 0.6680*ALD2 + 0.1170*RO2R + 0.1170*RO2 + 0.1834*HO2 + 0.0802*OH + 0.1859*CO	ARRW	0.664	1.32E-14	2105	0.336	9.08E-15	1137	
ALKE + O => 0.2656*CO + 0.3360*MEK + 0.2656*HCHO + 0.1328*ALD2 + 0.2672*HO2 + 0.3984*RO2R + 0.3984*RO2	ARRW	0.664	1.18E-11	324	0.336	2.26E-11	-10	
ALKE + NO3 => NO2 + 0.6640*HCHO + 1.3360*ALD2 + R2O2 + RO2	ARRW	0.664	5.00E-12	1935	0.336	1.00E-11	975	
TOLU + OH => 0.16*CRES + 0.16*HO2 + 0.84*RO2R + 0.4*DIAL + 0.84*RO2 + 0.144*MGLY + 0.114*HCHO + 0.114*CO	ARRH	2.10E-12	-322					

APPENDIX A –CHEMICAL TRANSFORMATION MECHANISMS

AROM + OH => 0.17*CRES + 0.17*HO2 + 0.83*RO2R + 0.83*RO2 + 0.6095*DIAL + 0.4539*MGLY + 0.0241*CO + 0.0129*HCHO	ARRW	0.7466	1.66E-11	-116	0.2534	6.20E-11	0
DIAL + OH => MCO3	CONS	3.00E-11					
DIAL => HO2 + CO + MCO3	PHOT	9	1				
CRES + OH => 0.2*MGLY + 0.15*RO2P + 0.85*RO2R + RO2	CONS	4.00E-11					
CRES + NO3 => HNO3 + BZO	CONS	2.19E-11					
RO2P + NO => NPHE	ARRH	4.20E-12	-180				
RO2P + HO2 => NR	CONS	3.00E-12					
RO2P + RO2 => 0.5*HO2 + RO2	CONS	1.00E-15					
RO2P + MCO3 => HCHO + HO2	CONS	3.00E-12					
BZO + NO2 => NPHE	CONS	1.50E-11					
BZO + HO2 => NR	CONS	3.00E-12					
BZO => NR	CONS	1.00E-03					
NPHE + NO3 => HNO3 + BZN2	CONS	3.81E-12					
BZN2 + NO2 => NR	CONS	1.50E-11					
BZN2 + HO2 => NPHE	CONS	3.00E-12					
BZN2 => NPHE	CONS	1.00E-03					
H2O2 => 2.0*OH	PHOT	4	0.255				
H2O2 + OH => HO2	ARRH	3.09E-12	187				
MEOH + OH => HCHO + HO2	TDAF	6.38E-18	2	-148			
CH4 + OH => HCHO + RO2 + RO2R	TDAF	6.95E-18	2	1282			
ISOP + OH => HCHO + ALD2 + RO2R + RO2	ARRH	2.54E-11	-410				

APPENDIX A –CHEMICAL TRANSFORMATION MECHANISMS

ISOP + O3 => 0.5*HCHO + 0.65*ALD2 + 0.21*MEK + 0.16*HO2 + 0.29*CO + 0.06*OH + 0.14*RO2R + 0.14*RO2	ARRH	1.23E-14	2013				
ISOP + O => 0.4*HO2 + 0.5*MEK + 0.5*ALD2	CONS	5.99E-11					
ISOP + NO3 => NO2 + HCHO + ALD2 + R2O2 + RO2	ARRH	2.54E-11	1121				
ETOH + OH => ALD2 + HO2	TDAF	6.17E-18	2	-532			
MTBE + 1.4*OH => 0.6*TBF + 0.4*HCHO + 0.4*MEK + 1.4*RO2R + 0.4*R2O2 + 1.8*RO2	TDAF	6.81E-18	2	-460			
SO2 + OH => SO3 + HO2	CONS	9.08E-13					

6. Carbon Bond 2005 mechanism

Mechanism name- CB05.

Reference

Yarwood G., Rao S., Yocke M., Whitten G., 2005. Updates to the Carbon Bond chemical mechanism.: CB05. Final report RT-04-00675 to U.S. Environmental Protection Agency, Research Triangle Park, NC 27703.

Table 20 Carbon Bond 2005 species listing.

Short Name	Long Name	de/ss	g/a	mw (g)
NO	'nitric oxide'	DE	g	30
NO2	'nitrogen dioxide'	DE	g	46
O3	'ozone'	DE	g	48
HO2	'hydroperoxy radical'	DE	g	33
H2O2	'hydrogen peroxide'	DE	g	36
O3	'nitrate radical'	DE	g	62
N2O5	'nitrogen pentoxide'	DE	g	108
HONO	'nitrous acid'	DE	g	47
HNO3	'nitric acid'	DE	g	63
PNA	'pernitric acid'	DE	g	79
CO	'carbon monoxide'	DE	g	28
FORM	'formaldehyde'	DE	g	30
ALD2	'acetaldehyde'	DE	g	44
C2O3	'acylperoxy radical'	DE	g	75
PAN	'peroxyacetyl nitrate'	DE	g	121
ALDX	'higher aldehyde'	DE	g	44

APPENDIX A –CHEMICAL TRANSFORMATION MECHANISMS

CXO3	'higher acylperoxy radical'	DE	g	75
PANX	'higher peroxyacyl nitrate'	DE	g	121
XO2	'NO-NO2 conversion from RO2'	DE	g	1
XO2N	'NO-org. nitrate conversion'	DE	g	1
NTR	'organic nitrate'	DE	g	130
ETOH	'ethanol'	DE	g	46
CH4	'methane'	DE	g	16
MEO2	'methylperoxy radical'	DE	g	47
MEOH	'methanol'	DE	g	32
MEPX	'methylhydroperoxide'	DE	g	48
FACD	'formic acid'	DE	g	46
ETHA	'ethane'	DE	g	30.1
ROOH	'higher organic peroxide'	DE	g	62
AACD	'higher carboxylic acid'	DE	g	60
PACD	'higher peroxy-carboxylic acid'	DE	g	76
HCO3	'bicarbonate ion'	DE	g	63
PAR	'parafin'	DE	g	14.32
ETH	'ethene'	DE	g	28
OLE	'terminal olefin carbon bond'	DE	g	28
IOLE	'internal olefin carbon bond'	DE	g	48
ISOP	'isoprene'	DE	g	68.1
ISPD	'isoprene product'	DE	g	70
TERP	'terpene'	DE	g	136
TOL	'toluene and monoalkyl arom.'	DE	g	92
XYL	'xylene and polyalkyl arom.'	DE	g	106
CRES	'cresole and high m.w.phenols'	DE	g	108.1
OPEN	'arom. ring opening prods'	DE	g	100
MGLY	'methylglyxl and arom. prods'	DE	g	72
O1D	'oxygen singlet D'	SS	g	1
OH	'hydroxy radical'	SS	g	1
O	'oxygen singlet P'	SS	g	1
ROR	'radical'	SS	g	1
TO2	'radical'	SS	g	1

APPENDIX A –CHEMICAL TRANSFORMATION MECHANISMS

CRO	'radical'	SS	g	1
SO2	'sulfur dioxide'	DE	g	64.1
SO3	'sulfuric acid'	DE	g	98.1

Table 21 Carbon Bond 2005 reactions.

REACTION	RATE	VARIABLE					
NO2 => NO + O	PHOT	1	1				
O + O2 + M => O3 + M	TDCN	6.00E-34	-2.4				
O3 + NO => NO2	ARRH	3.00E-12	1500				
O + NO2 => NO	ARRH	5.60E-12	-180				
O + NO2 => NO3	TROE	2.50E-31	-1.8	2.20E-11	-0.7	0.6	
O + NO => NO2	TROE	9.00E-32	-1.5	3.00E-11	0	0.6	
O3 + NO2 => NO3	ARRH	1.20E-13	2450				
O3 => O	PHOT	10	1				
O3 => O1D	PHOT	2	1				
O1D + M => O + M	ARRH	2.10E-11	-102				
O1D + H2O => 2.0*OH	CONS	2.20E-10					
O3 + OH => HO2	ARRH	1.70E-12	940				
O3 + HO2 => OH	ARRH	1.00E-14	490				
NO3 => NO2 + O	PHOT	11	1				
NO3 => NO	PHOT	8	1				
NO + NO3 => 2.0*NO2	ARRH	1.50E-11	-170				

APPENDIX A –CHEMICAL TRANSFORMATION MECHANISMS

NO2 + NO3 => NO + NO2	ARRH	4.50E-14	1260					
NO2 + NO3 => N2O5	TROE	2.00E-30	-4.4	1.40E-12	-0.7	0.6		
N2O5 + H2O => 2.0*HNO3	CONS	2.50E-22						
N2O5 + H2O + H2O => 2*HNO3	CONS	1.80E-39						
N2O5 => NO2 + NO3	FALL	1.00E-03	-3.5	11000	9.70E+14	0.1	11080	0.45
NO + NO + O2 => 2.0*NO2	ARRH	3.30E-39	-530					
NO + NO2 + H2O => 2.0*HONO	CONS	5.00E-40						
NO + OH => HONO	TROE	7.00E-31	-2.6	3.60E-11	-0.1	0.6		
HONO => NO + OH	PHOT	12	1					
OH + HONO => NO2	ARRH	1.80E-11	390					
HONO + HONO => NO + NO2	CONS	1.00E-20						
OH + NO2 => HNO3	TROE	2.00E-30	-3	2.50E-11	0	0.6		
OH + HNO3 => NO3	LMHW	2.40E-14	-460	2.70E-17	-2199	6.50E-34	-1335	
NO + HO2 => OH + NO2	ARRH	3.50E-12	-250					
NO2 + HO2 => PNA	TROE	1.80E-31	-3.2	4.70E-12	0	0.6		
PNA => NO2 + HO2	FALL	4.10E-05	0	10650	4.80E+15	0	11170	0.6
OH + PNA => NO2	ARRH	1.30E-12	-380					
HO2 + HO2 => H2O2	ARRM	2.30E-13	-600	1.70E-33	-1000			
HO2 + HO2 + H2O => H2O2	ARRM	3.22E-34	-2800	2.38E-54	-3200			
H2O2 => 2.0*OH	PHOT	13	1					
H2O2 + OH => HO2	ARRH	2.90E-12	160					

APPENDIX A –CHEMICAL TRANSFORMATION MECHANISMS

O1D + H2 => OH + HO2	CONS	1.10E-10					
OH + H2 => HO2	ARRH	5.50E-12	2000				
OH + O => HO2	ARRH	2.20E-11	-120				
OH + OH => O	ARRH	4.20E-12	240				
OH + OH => H2O2	TROE	6.90E-31	-1	2.60E-11	0	0.6	
OH + HO2 => NR	ARRH	4.80E-11	-250				
HO2 + O => OH	ARRH	3.00E-11	-200				
H2O2 + O => OH + HO2	ARRH	1.40E-12	2000				
NO3+ O => NO2	CONS	1.00E-11					
NO3 + OH => HO2 + NO2	CONS	2.20E-11					
NO3 + HO2 => HNO3	CONS	3.50E-12					
NO3 + O3 => NO2	CONS	1.00E-17					
NO3 + NO3 => 2*NO2	ARRH	8.50E-13	2450				
PNA => 0.61*HO2 + 0.61*NO2 +0.39*OH +0.39*NO3	PHOT	14	1				
HNO3 => OH + NO2	PHOT	15	1				
N2O5 => NO2 + NO3	PHOT	16	1				
XO2 + NO => NO2	ARRH	2.60E-12	-365				
XO2N + NO => NTR	ARRH	2.60E-12	-365				
XO2 + HO2 => ROOH	ARRH	7.50E-13	-700				
XO2N + HO2 => ROOH	ARRH	7.50E-13	-700				
XO2 + XO2 => NR	CONS	6.80E-14					

APPENDIX A –CHEMICAL TRANSFORMATION MECHANISMS

XO2N + XO2N => NR	CONS	6.80E-14					
XO2N + XO2 => NR	CONS	6.80E-14					
NTR + OH => HNO3 + HO2 + 0.33*FORM + 0.33*ALD2 + 0.33*ALDX - 0.66*PAR	ARRH	5.90E-13	360				
NTR => NO2 + HO2 + 0.33*FORM + 0.33*ALD2 + 0.33*ALDX - 0.66*PAR	PHOT	17	1				
ROOH + OH => XO2 + 0.50*ALD2 + 0.50*ALDX	ARRH	3.01E-12	-190				
ROOH => OH + HO2 + 0.50*ALD2 + 0.50*ALDX	PHOT	18	1				
OH + CO => HO2	ARRM	1.44E-13	0	3.43E-33	0		
OH + CH4 => MEO2	ARRH	2.45E-12	1775				
MEO2 + NO => FORM + HO2 + NO2	ARRH	2.80E-12	-300				
MEO2 + HO2 => MEPX	ARRH	4.10E-13	-750				
MEO2 + MEO2 => 1.37*FORM + 0.74*HO2 + 0.63*MEOH	ARRH	9.50E-14	-390				
MEPX + OH => 0.70*MEO2 + 0.30*XO2 + 0.30*HO2	ARRH	3.80E-12	-200				
MEPX => FORM + HO2 + OH	PHOT	18	1				
MEOH + OH => FORM + HO2	ARRH	7.30E-12	620				
FORM + OH => HO2 + CO	CONS	9.00E-12					
FORM => 2*HO2 + CO	PHOT	3	1				
FORM => CO	PHOT	4	1				
FORM + O => OH + HO2 + CO	ARRH	3.40E-11	1600				
FORM + NO3 => HNO3 + HO2 + CO	CONS	5.80E-16					
FORM + HO2 => HCO3	ARRH	9.70E-15	-625				
HCO3 => FORM + HO2	ARRH	2.40E+12	7000				

APPENDIX A –CHEMICAL TRANSFORMATION MECHANISMS

HCO3 + NO => FACD + NO2 + HO2	CONS	5.60E-12						
HCO3 + HO2 => MEPX	ARRH	5.60E-15	-2300					
FACD + OH => HO2	CONS	4.00E-13						
ALD2 + O => C2O3 + OH	ARRH	1.80E-11	1100					
ALD2 + OH => C2O3	ARRH	5.60E-12	-270					
ALD2 + NO3 => C2O3 + HNO3	ARRH	1.40E-12	1900					
ALD2 => MEO2 + CO + HO2	PHOT	5	1					
C2O3 + NO => MEO2 + NO2	ARRH	8.10E-12	-270					
C2O3 + NO2 => PAN	TROE	2.70E-28	-7.1	1.20E-11	-0.9	0.3		
PAN => C2O3 + NO2	FALL	4.90E-03	0	12100	5.40E+16	0	13830	0.3
PAN => C2O3 + NO2	PHOT	19	1					
C2O3 + HO2 => 0.80*PACD + 0.20*AACD + 0.20*O3	ARRH	4.30E-13	-1040					
C2O3 + MEO2 => 0.90*MEO2 + 0.90*HO2 + FORM + 0.10*AACD	ARRH	2.00E-12	-500					
C2O3 + XO2 => 0.90*MEO2 + 0.10*AACD	ARRH	4.40E-13	-1070					
C2O3 + C2O3 => 2*MEO2	ARRH	2.90E-12	-500					
PACD + OH => C2O3	ARRH	4.00E-13	-200					
PACD => MEO2 + OH	PHOT	18	1					
AACD + OH => MEO2	ARRH	4.00E-13	-200					
ALDX + O => CXO3 + OH	ARRH	1.30E-11	870					
ALDX + OH => CXO3	ARRH	5.10E-12	-405					
ALDX + NO3 => CXO3 + HNO3	CONS	6.50E-15						

APPENDIX A –CHEMICAL TRANSFORMATION MECHANISMS

ALDX => MEO2 + CO + HO2	PHOT	20	1					
CXO3 + NO => ALD2 + NO2 + HO2 + XO2	ARRH	6.70E-12	-340					
CXO3 + NO2 => PANX	TROE	2.70E-28	-7.1	1.20E-11	-0.9	0.3		
PANX => CXO3 + NO2	FALL	4.90E-03	0	12100	5.40E+16	0	13830	0.3
PANX => CXO3 + NO2	PHOT	19	1					
PANX + OH => ALD2 + NO2	CONS	3.00E-13						
CXO3 + HO2 => 0.80*PACD + 0.20*AACD + 0.20*O3	ARRH	4.30E-13	-1040					
CXO3 + MEO2 => 0.90*ALD2 + 0.90*XO2 + HO2 + 0.10*AACD + 0.10*FORM	ARRH	2.00E-12	-500					
CXO3 + XO2 => 0.90*ALD2 + 0.10*AACD	ARRH	4.40E-13	-1070					
CXO3 + CXO3 => 2*ALD2 + 2*XO2 + 2*HO2	ARRH	2.90E-12	-500					
CXO3 + C2O3 => MEO2 + XO2 + HO2 + ALD2	ARRH	2.90E-12	-500					
PAR + OH => 0.87*XO2 + 0.13*XO2N + 0.11*HO2 + 0.06*ALD2 - 0.11*PAR + 0.76*ROR + 0.05*ALDX	CONS	8.10E-13						
ROR => 0.96*XO2 + 0.60*ALD2 + 0.94*HO2 - 2.10*PAR + 0.04*XO2N + 0.02*ROR + 0.5*ALDX	ARRH	1.00E+15	8000					
ROR => HO2	CONS	1.60E+03						
ROR + NO2 => NTR	CONS	1.50E-11						
O + OLE => 0.2*ALD2 + 0.3*ALDX + 0.3*HO2 + 0.2*XO2 + 0.20*CO + 0.20*FORM + 0.01*XO2N + 0.2*PAR + 0.10*OH	ARRH	1.00E-11	280					
OH + OLE => 0.8*FORM + 0.33*ALD2 + 0.62*ALDX + 0.8*XO2 + 0.95*HO2 - 0.70*PAR	CONS	3.20E-11						
O3 + OLE => 0.18*ALD2 + 0.74*FORM + 0.32*ALDX + 0.22*XO2 + 0.1*OH + 0.33*CO + 0.44*HO2 - 1.0*PAR	ARRH	6.50E-15	1900					
NO3 + OLE => NO2 + FORM + 0.91*XO2 + 0.09*XO2N + 0.56*ALDX + 0.35*ALD2 - 1.0*PAR	ARRH	7.00E-13	2160					

APPENDIX A –CHEMICAL TRANSFORMATION MECHANISMS

O + ETH => FORM + 1.7*HO2 + CO + 0.7*XO2 + 0.3*OH	ARRH	1.04E-11	792					
OH + ETH => XO2 + 1.56*FORM + HO2 + 0.22*ALDX	TROE	1.00E-28	-0.8	8.80E-12	0	0.6		
O3 + ETH => FORM + 0.63*CO + 0.13*HO2 + 0.13*OH + 0.37*FACD	ARRH	1.20E-14	2630					
NO3 + ETH => NO2 + XO2 + 2*FORM	ARRH	3.30E-12	2880					
IOLE + O => 1.24*ALD2 + 0.66*ALDX + 0.10*HO2 + 0.1*XO2 + 0.1*CO + 0.1*PAR	CONS	2.30E-11						
IOLE + OH => 1.3*ALD2 + 0.7*ALDX + HO2 + XO2	ARRH	1.00E-11	-550					
IOLE + O3 => 0.65*ALD2 + 0.35*ALDX + 0.25*FORM + 0.25*CO + 0.50*O + 0.50*OH + 0.5*HO2	ARRH	8.40E-15	1100					
IOLE + NO3 => 1.18*ALD2 + 0.64*ALDX + HO2 + NO2	ARRH	9.60E-13	270					
TOL + OH => 0.440*HO2 + 0.080*XO2 + 0.360*CRES + 0.560*TO2	ARRH	1.80E-12	-355					
TO2 + NO => 0.900*NO2 + 0.900*HO2 + 0.900*OPEN + 0.100*NTR	CONS	8.10E-12						
TO2 => CRES + HO2	CONS	4.2						
OH + CRES => 0.400*CRO + 0.600*XO2 + 0.600*HO2 + 0.300*OPEN	CONS	4.10E-11						
CRES + NO3 => CRO + HNO3	CONS	2.20E-11						
CRO + NO2 => NTR	CONS	1.40E-11						
CRO + HO2 => CRES	CONS	5.50E-12						
OPEN => C2O3 + HO2 + CO	PHOT	3	9					
OPEN + OH => XO2 + 2.000*CO + 2.00*HO2 + C2O3 + FORM	CONS	3.00E-11						
OPEN + O3 => 0.030*ALDX + 0.620*C2O3 + 0.700*FORM + 0.030*XO2 + 0.690*CO + 0.080*OH + 0.760*HO2 + 0.200*MGLY	ARRH	5.40E-17	500					
OH + XYL => 0.700*HO2 + 0.500*XO2 + 0.200*CRES + 0.800*MGLY + 1.100*PAR + 0.300*TO2	ARRH	1.70E-11	-116					
OH + MGLY => XO2 + C2O3	CONS	1.80E-11						

APPENDIX A –CHEMICAL TRANSFORMATION MECHANISMS

MGLY => C2O3 + HO2 + CO	PHOT	21	1				
O + ISOP => 0.750*ISPD + 0.500*FORM + 0.250*XO2 + 0.250*HO2 + 0.250*CXO3 + 0.250*PAR	CONS	3.60E-11					
OH + ISOP => 0.912*ISPD + 0.629*FORM + 0.991*XO2 + 0.912*HO2 + 0.088*XO2N	ARRH	2.54E-11	-407.6				
O3 + ISOP => 0.650*ISPD + 0.600*FORM + 0.200*XO2 + 0.066*HO2 + 0.266*OH + 0.200*CXO3 + 0.150*ALDX + 0.350*PAR + 0.066*CO	ARRH	7.86E-15	1912				
NO3 + ISOP => 0.200*ISPD + 0.800*NTR + XO2 + 0.800*HO2 + 0.200*NO2 + 0.800*ALDX + 2.400*PAR	ARRH	3.03E-12	448				
OH + ISPD => 1.565*PAR + 0.167*FORM + 0.713*XO2 + 0.503*HO2 + 0.334*CO + 0.168*MGLY + 0.252*ALD2 + 0.210*C2O3 + 0.250*CXO3 + 0.120*ALDX	CONS	3.36E-11					
O3 + ISPD => 0.114*C2O3 + 0.150*FORM + 0.850*MGLY + 0.154*HO2 + 0.268*OH + 0.064*XO2 + 0.020*ALD2 + 0.360*PAR + 0.225*CO	CONS	7.10E-18					
NO3 + ISPD => 0.357*ALDX + 0.282*FORM + 1.282*PAR + 0.925*HO2 + 0.643*CO + 0.850*NTR + 0.075*CXO3 + 0.075*XO2 + 0.150*HNO3	CONS	1.00E-15					
ISPD => 0.333*CO + 0.067*ALD2 + 0.900*FORM + 0.832*PAR + 1.033*HO2 + 0.700*XO2 + 0.967*C2O3	PHOT	22	0.0034				
TERP + O => 0.150*ALDX + 5.12*PAR	CONS	3.60E-11					
TERP + OH => 0.750*HO2 + 1.250*XO2 + 0.250*XO2N + 0.280*FORM + 1.66*PAR + 0.470*ALDX	ARRH	1.50E-11	-449				
TERP + O3 => 0.570*OH + 0.070*HO2 + 0.760*XO2 + 0.180*XO2N + 0.240*FORM + 0.001*CO + 7.000*PAR + 0.210*ALDX + 0.390*CXO3	ARRH	1.20E-15	821				
TERP + NO3 => 0.470*NO2 + 0.280*HO2 + 1.030*XO2 + 0.250*XO2N + 0.470*ALDX + 0.530*NTR	ARRH	3.70E-12	-175				
SO2 + OH => SO3 + HO2	TROE	3.00E-31	-3.3	1.50E-12	0	0.6	
OH + ETOH => HO2 + 0.900*ALD2 + 0.050*ALDX + 0.100*FORM + 0.100*XO2	ARRH	6.90E-12	230				

OH + ETHA => 0.991*ALD2 + 0.991*XO2 + 0.009*XO2N + HO2	ARRH	8.70E-12	1070						
NO2 + ISOP => 0.200*ISPD + 0.800*NTR + XO2 + 0.800*HO2 + 0.200*NO + 0.800*ALDX + 2.400*PAR	CONS	1.50E-19							

7. Carbon Bond 2005 mechanism + aerosols

Mechanism name: CB05_AER.

Reference

Yarwood G., Rao S., Yocke M., Whitten G., 2005. Updates to the Carbon Bond chemical mechanism.: CB05. Final report RT-04-00675 to U.S. Environmental Protection Agency, Research Triangle Park, NC 27703.

Table 22 Carbon Bond + aerosol species listing

Short Name	Long Name	de/ss	g/a	mw (g)
NO	'nitric oxide'	DE	g	30
NO2	'nitrogen dioxide'	DE	g	46
O3	'ozone'	DE	g	48
HO2	'hydroperoxy radical'	DE	g	33
H2O2	'hydrogen peroxide'	DE	g	36
O3	'nitrate radical'	DE	g	62
N2O5	'nitrogen pentoxide'	DE	g	108
HONO	'nitrous acid'	DE	g	47
HNO3	'nitric acid'	DE	g	63
PNA	'pernitric acid'	DE	g	79
CO	'carbon monoxide'	DE	g	28
FORM	'formaldehyde'	DE	g	30
ALD2	'acetaldehyde'	DE	g	44
C2O3	'acylperoxy radical'	DE	g	75
PAN	'peroxyacetyl nitrate'	DE	g	121
ALDX	'higher aldehyde'	DE	g	44

APPENDIX A –CHEMICAL TRANSFORMATION MECHANISMS

CXO3	'higher acylperoxy radical'	DE	g	75
PANX	'higher peroxyacyl nitrate'	DE	g	121
XO2	'NO-NO2 conversion from RO2'	DE	g	1
XO2N	'NO-org. nitrate conversion'	DE	g	1
NTR	'organic nitrate'	DE	g	130
ETOH	'ethanol'	DE	g	46
CH4	'methane'	DE	g	16
MEO2	'methylperoxy radical'	DE	g	47
MEOH	'methanol'	DE	g	32
MEPX	'methylhydroperoxide'	DE	g	48
FACD	'formic acid'	DE	g	46
ETHA	'ethane'	DE	g	30.1
ROOH	'higher organic peroxide'	DE	g	62
AACD	'higher carboxylic acid'	DE	g	60
PACD	'higher peroxy-carboxylic acid'	DE	g	76
HCO3	'bicarbonate ion'	DE	g	63
PAR	'parafin'	DE	g	14.32
ETH	'ethene'	DE	g	28
OLE	'terminal olefin carbon bond'	DE	g	28
IOLE	'internal olefin carbon bond'	DE	g	48
ISOP	'isoprene'	DE	g	68.1
ISPD	'isoprene product'	DE	g	70
TERP	'terpene'	DE	g	136
TOL	'toluene and monoalkyl arom.'	DE	g	92
XYL	'xylene and polyalkyl arom.'	DE	g	106
CRES	'cresole and high m.w.phenols'	DE	g	108.1
OPEN	'arom. ring opening prods'	DE	g	100
MGLY	'methylglyxl and arom. prods'	DE	g	72
O1D	'oxygen singlet D'	SS	g	1
OH	'hydroxy radical'	SS	g	1
O	'oxygen singlet P'	SS	g	1
ROR	'radical'	SS	g	1
TO2	'radical'	SS	g	1

APPENDIX A –CHEMICAL TRANSFORMATION MECHANISMS

CRO	'radical'	SS	g	1
SO2	'sulfur dioxide'	DE	g	64.1
SO3	'sulfuric acid'	DE	g	98.1
NH3	'ammonia'	DE	g	17
NH4	'ammonium ions'	DE	a	18
NIT	'aerosol nitrate'	DE	a	62
SO2	'sulfur dioxide'	DE	g	64.1
SO3	'sulfuric acid'	DE	g	98.1
ASO4	'aerosol sulfate (<2.5um)'	DE	a	96.1
AS10	'aerosol sulfate (2.5-10 um)'	DE	a	96.1
WPER	'dissolved hydrogen peroxide'	DE	g	36
WNIT	'dissolved nitric acid'	DE	g	63
WSO4	'sulfate ions in cloud water'	DE	a	96.1
RSO4	'sulfate ions in rain water'	DE	a	96.1
OC25	'PM2.5 organic carbon'	DE	a	1
OC10	'PM2.5-10 organic carbon'	DE	a	1
EC25	'PM2.5 elemental carbon'	DE	a	1
EC10	'PM2-10 elemental carbon'	DE	a	1
OT25	'PM2.5 miscellaneous'	DE	a	1
OT10	'PM2.5-10 miscellaneous'	DE	a	1
SS25	'PM2.5 sea salt'	DE	a	1
SS10	'PM2.5-10 sea salt'	DE	a	1
CG1	'OLE condensable gas 1'	DE	g	140
CG2	'OLE condensable gas 2'	DE	g	140
CG3	'PAR condensable gas'	DE	g	140
CG4	'XYL condensable gas 1'	DE	g	150
CG5	'XYL condensable gas 2'	DE	g	150
CG6	'TOL condensable gas 1'	DE	g	150
CG7	'TOL condensable gas 2'	DE	g	150
CG8	'TERP condensable gas 1'	DE	g	184
CG9	'TERP condensable gas 2'	DE	g	184
CG10	'TERP condensable gas 3'	DE	g	184

APPENDIX A –CHEMICAL TRANSFORMATION MECHANISMS

CG11	'TERP condensable gas 4'	DE	g	184
CG12	'ISO condensable gas 1'	DE	g	150
CG13	'ISO condensable gas 2'	DE	g	150
SOL1	'Olefin SOA 1'	DE	a	1
SOL2	'Olefin SOA 2'	DE	a	1
SPAR	'Paraffin SOA 1'	DE	a	1
SXY1	'Xylene SOA 1'	DE	a	1
SXY2	'Xylene SOA 2'	DE	a	1
STO1	'Toluene SOA 1'	DE	a	1
STO2	'Toluene SOA 2'	DE	a	1
STE1	'Terpene SOA 1'	DE	a	1
STE2	'Terpene SOA 2'	DE	a	1
STE3	'Terpene SOA 3'	DE	a	1
STE4	'Terpene SOA 4'	DE	a	1
SIS1	'Isoprene SOA 1'	DE	a	1
SIS2	'Isoprene SOA 2'	DE	a	1
NSOA	'Non-volatile SOA'	DE	a	1
SIS1	'Isoprene SOA 1'	DE	a	1

APPENDIX A –CHEMICAL TRANSFORMATION MECHANISMS

Table 23 Carbon Bond 2005 + aerosol mechanism

REACTION	RATE	VARIABLE					
NO2 => NO + O	PHOT	1	1				
O + O2 + M => O3 + M	TDCN	6.00E-34	-2.4				
O3 + NO => NO2	ARRH	3.00E-12	1500				
O + NO2 => NO	ARRH	5.60E-12	-180				
O + NO2 => NO3	TROE	2.50E-31	-1.8	2.20E-11	-0.7	0.6	
O + NO => NO2	TROE	9.00E-32	-1.5	3.00E-11	0	0.6	
O3 + NO2 => NO3	ARRH	1.20E-13	2450				
O3 => O	PHOT	10	1				
O3 => O1D	PHOT	2	1				
O1D + M => O + M	ARRH	2.10E-11	-102				
O1D + H2O => 2.0*OH	CONS	2.20E-10					
O3 + OH => HO2	ARRH	1.70E-12	940				
O3 + HO2 => OH	ARRH	1.00E-14	490				
NO3 => NO2 + O	PHOT	11	1				
NO3 => NO	PHOT	8	1				
NO + NO3 => 2.0*NO2	ARRH	1.50E-11	-170				

APPENDIX A –CHEMICAL TRANSFORMATION MECHANISMS

NO2 + NO3 => NO + NO2	ARRH	4.50E-14	1260					
NO2 + NO3 => N2O5	TROE	2.00E-30	-4.4	1.40E-12	-0.7	0.6		
N2O5 + H2O => 2.0*HNO3	CONS	2.50E-22						
N2O5 + H2O + H2O => 2*HNO3	CONS	1.80E-39						
N2O5 => NO2 + NO3	FALL	1.00E-03	-3.5	11000	9.70E+14	0.1	11080	0.45
NO + NO + O2 => 2.0*NO2	ARRH	3.30E-39	-530					
NO + NO2 + H2O => 2.0*HONO	CONS	5.00E-40						
NO + OH => HONO	TROE	7.00E-31	-2.6	3.60E-11	-0.1	0.6		
HONO => NO + OH	PHOT	12	1					
OH + HONO => NO2	ARRH	1.80E-11	390					
HONO + HONO => NO + NO2	CONS	1.00E-20						
OH + NO2 => HNO3	TROE	2.00E-30	-3	2.50E-11	0	0.6		
OH + HNO3 => NO3	LMHW	2.40E-14	-460	2.70E-17	-2199	6.50E-34	-1335	
NO + HO2 => OH + NO2	ARRH	3.50E-12	-250					
NO2 + HO2 => PNA	TROE	1.80E-31	-3.2	4.70E-12	0	0.6		
PNA => NO2 + HO2	FALL	4.10E-05	0	10650	4.80E+15	0	11170	0.6
OH + PNA => NO2	ARRH	1.30E-12	-380					
HO2 + HO2 => H2O2	ARRM	2.30E-13	-600	1.70E-33	-1000			
HO2 + HO2 + H2O => H2O2	ARRM	3.22E-34	-2800	2.38E-54	-3200			
H2O2 => 2.0*OH	PHOT	13	1					
H2O2 + OH => HO2	ARRH	2.90E-12	160					

APPENDIX A –CHEMICAL TRANSFORMATION MECHANISMS

O1D + H2 => OH + HO2	CONS	1.10E-10					
OH + H2 => HO2	ARRH	5.50E-12	2000				
OH + O => HO2	ARRH	2.20E-11	-120				
OH + OH => O	ARRH	4.20E-12	240				
OH + OH => H2O2	TROE	6.90E-31	-1	2.60E-11	0	0.6	
OH + HO2 => NR	ARRH	4.80E-11	-250				
HO2 + O => OH	ARRH	3.00E-11	-200				
H2O2 + O => OH + HO2	ARRH	1.40E-12	2000				
NO3+ O => NO2	CONS	1.00E-11					
NO3 + OH => HO2 + NO2	CONS	2.20E-11					
NO3 + HO2 => HNO3	CONS	3.50E-12					
NO3 + O3 => NO2	CONS	1.00E-17					
NO3 + NO3 => 2*NO2	ARRH	8.50E-13	2450				
PNA => 0.61*HO2 + 0.61*NO2 +0.39*OH +0.39*NO3	PHOT	14	1				
HNO3 => OH + NO2	PHOT	15	1				
N2O5 => NO2 + NO3	PHOT	16	1				
XO2 + NO => NO2	ARRH	2.60E-12	-365				
XO2N + NO => NTR	ARRH	2.60E-12	-365				
XO2 + HO2 => ROOH	ARRH	7.50E-13	-700				
XO2N + HO2 => ROOH	ARRH	7.50E-13	-700				
XO2 + XO2 => NR	CONS	6.80E-14					

APPENDIX A –CHEMICAL TRANSFORMATION MECHANISMS

XO2N + XO2N => NR	CONS	6.80E-14					
XO2N + XO2 => NR	CONS	6.80E-14					
NTR + OH => HNO3 + HO2 + 0.33*FORM + 0.33*ALD2 + 0.33*ALDX - 0.66*PAR	ARRH	5.90E-13	360				
NTR => NO2 + HO2 + 0.33*FORM + 0.33*ALD2 + 0.33*ALDX - 0.66*PAR	PHOT	17	1				
ROOH + OH => XO2 + 0.50*ALD2 + 0.50*ALDX	ARRH	3.01E-12	-190				
ROOH => OH + HO2 + 0.50*ALD2 + 0.50*ALDX	PHOT	18	1				
OH + CO => HO2	ARRM	1.44E-13	0	3.43E-33	0		
OH + CH4 => MEO2	ARRH	2.45E-12	1775				
MEO2 + NO => FORM + HO2 + NO2	ARRH	2.80E-12	-300				
MEO2 + HO2 => MEPX	ARRH	4.10E-13	-750				
MEO2 + MEO2 => 1.37*FORM + 0.74*HO2 + 0.63*MEOH	ARRH	9.50E-14	-390				
MEPX + OH => 0.70*MEO2 + 0.30*XO2 + 0.30*HO2	ARRH	3.80E-12	-200				
MEPX => FORM + HO2 + OH	PHOT	18	1				
MEOH + OH => FORM + HO2	ARRH	7.30E-12	620				
FORM + OH => HO2 + CO	CONS	9.00E-12					
FORM => 2*HO2 + CO	PHOT	3	1				
FORM => CO	PHOT	4	1				
FORM + O => OH + HO2 + CO	ARRH	3.40E-11	1600				
FORM + NO3 => HNO3 + HO2 + CO	CONS	5.80E-16					
FORM + HO2 => HCO3	ARRH	9.70E-15	-625				
HCO3 => FORM + HO2	ARRH	2.40E+12	7000				

APPENDIX A –CHEMICAL TRANSFORMATION MECHANISMS

HCO3 + NO => FACD + NO2 + HO2	CONS	5.60E-12						
HCO3 + HO2 => MEPX	ARRH	5.60E-15	-2300					
FACD + OH => HO2	CONS	4.00E-13						
ALD2 + O => C2O3 + OH	ARRH	1.80E-11	1100					
ALD2 + OH => C2O3	ARRH	5.60E-12	-270					
ALD2 + NO3 => C2O3 + HNO3	ARRH	1.40E-12	1900					
ALD2 => MEO2 + CO + HO2	PHOT	5	1					
C2O3 + NO => MEO2 + NO2	ARRH	8.10E-12	-270					
C2O3 + NO2 => PAN	TROE	2.70E-28	-7.1	1.20E-11	-0.9	0.3		
PAN => C2O3 + NO2	FALL	4.90E-03	0	12100	5.40E+16	0	13830	0.3
PAN => C2O3 + NO2	PHOT	19	1					
C2O3 + HO2 => 0.80*PACD + 0.20*AACD + 0.20*O3	ARRH	4.30E-13	-1040					
C2O3 + MEO2 => 0.90*MEO2 + 0.90*HO2 + FORM + 0.10*AACD	ARRH	2.00E-12	-500					
C2O3 + XO2 => 0.90*MEO2 + 0.10*AACD	ARRH	4.40E-13	-1070					
C2O3 + C2O3 => 2*MEO2	ARRH	2.90E-12	-500					
PACD + OH => C2O3	ARRH	4.00E-13	-200					
PACD => MEO2 + OH	PHOT	18	1					
AACD + OH => MEO2	ARRH	4.00E-13	-200					
ALDX + O => CXO3 + OH	ARRH	1.30E-11	870					
ALDX + OH => CXO3	ARRH	5.10E-12	-405					
ALDX + NO3 => CXO3 + HNO3	CONS	6.50E-15						

APPENDIX A –CHEMICAL TRANSFORMATION MECHANISMS

ALDX => MEO2 + CO + HO2	PHOT	20	1					
CXO3 + NO => ALD2 + NO2 + HO2 + XO2	ARRH	6.70E-12	-340					
CXO3 + NO2 => PANX	TROE	2.70E-28	-7.1	1.20E-11	-0.9	0.3		
PANX => CXO3 + NO2	FALL	4.90E-03	0	12100	5.40E+16	0	13830	0.3
PANX => CXO3 + NO2	PHOT	19	1					
PANX + OH => ALD2 + NO2	CONS	3.00E-13						
CXO3 + HO2 => 0.80*PACD + 0.20*AACD + 0.20*O3	ARRH	4.30E-13	-1040					
CXO3 + MEO2 => 0.90*ALD2 + 0.90*XO2 + HO2 + 0.10*AACD + 0.10*FORM	ARRH	2.00E-12	-500					
CXO3 + XO2 => 0.90*ALD2 + 0.10*AACD	ARRH	4.40E-13	-1070					
CXO3 + CXO3 => 2*ALD2 + 2*XO2 + 2*HO2	ARRH	2.90E-12	-500					
CXO3 + C2O3 => MEO2 + XO2 + HO2 + ALD2	ARRH	2.90E-12	-500					
PAR + OH => 0.87*XO2 + 0.13*XO2N + 0.11*HO2 + 0.06*ALD2 - 0.11*PAR + 0.76*ROR + 0.05*ALDX	CONS	8.10E-13						
ROR => 0.96*XO2 + 0.60*ALD2 + 0.94*HO2 - 2.10*PAR + 0.04*XO2N + 0.02*ROR + 0.5*ALDX	ARRH	1.00E+15	8000					
ROR => HO2	CONS	1.60E+03						
ROR + NO2 => NTR	CONS	1.50E-11						
O + OLE => 0.2*ALD2 + 0.3*ALDX + 0.3*HO2 + 0.2*XO2 + 0.20*CO + 0.20*FORM + 0.01*XO2N + 0.2*PAR + 0.10*OH	ARRH	1.00E-11	280					
OH + OLE => 0.8*FORM + 0.33*ALD2 + 0.62*ALDX + 0.8*XO2 + 0.95*HO2 - 0.70*PAR	CONS	3.20E-11						
O3 + OLE => 0.18*ALD2 + 0.74*FORM + 0.32*ALDX + 0.22*XO2 + 0.1*OH + 0.33*CO + 0.44*HO2 - 1.0*PAR	ARRH	6.50E-15	1900					
NO3 + OLE => NO2 + FORM + 0.91*XO2 + 0.09*XO2N + 0.56*ALDX + 0.35*ALD2 - 1.0*PAR	ARRH	7.00E-13	2160					

APPENDIX A –CHEMICAL TRANSFORMATION MECHANISMS

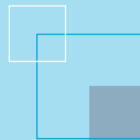
O + ETH => FORM + 1.7*HO2 + CO + 0.7*XO2 + 0.3*OH	ARRH	1.04E-11	792					
OH + ETH => XO2 + 1.56*FORM + HO2 + 0.22*ALDX	TROE	1.00E-28	-0.8	8.80E-12	0	0.6		
O3 + ETH => FORM + 0.63*CO + 0.13*HO2 + 0.13*OH + 0.37*FACD	ARRH	1.20E-14	2630					
NO3 + ETH => NO2 + XO2 + 2*FORM	ARRH	3.30E-12	2880					
IOLE + O => 1.24*ALD2 + 0.66*ALDX + 0.10*HO2 + 0.1*XO2 + 0.1*CO + 0.1*PAR	CONS	2.30E-11						
IOLE + OH => 1.3*ALD2 + 0.7*ALDX + HO2 + XO2	ARRH	1.00E-11	-550					
IOLE + O3 => 0.65*ALD2 + 0.35*ALDX + 0.25*FORM + 0.25*CO + 0.50*O + 0.50*OH + 0.5*HO2	ARRH	8.40E-15	1100					
IOLE + NO3 => 1.18*ALD2 + 0.64*ALDX + HO2 + NO2	ARRH	9.60E-13	270					
TOL + OH => 0.440*HO2 + 0.080*XO2 + 0.360*CRES + 0.560*TO2	ARRH	1.80E-12	-355					
TO2 + NO => 0.900*NO2 + 0.900*HO2 + 0.900*OPEN + 0.100*NTR	CONS	8.10E-12						
TO2 => CRES + HO2	CONS	4.2						
OH + CRES => 0.400*CRO + 0.600*XO2 + 0.600*HO2 + 0.300*OPEN	CONS	4.10E-11						
CRES + NO3 => CRO + HNO3	CONS	2.20E-11						
CRO + NO2 => NTR	CONS	1.40E-11						
CRO + HO2 => CRES	CONS	5.50E-12						
OPEN => C2O3 + HO2 + CO	PHOT	3	9					
OPEN + OH => XO2 + 2.000*CO + 2.00*HO2 + C2O3 + FORM	CONS	3.00E-11						
OPEN + O3 => 0.030*ALDX + 0.620*C2O3 + 0.700*FORM + 0.030*XO2 + 0.690*CO + 0.080*OH + 0.760*HO2 + 0.200*MGLY	ARRH	5.40E-17	500					
OH + XYL => 0.700*HO2 + 0.500*XO2 + 0.200*CRES + 0.800*MGLY + 1.100*PAR + 0.300*TO2	ARRH	1.70E-11	-116					
OH + MGLY => XO2 + C2O3	CONS	1.80E-11						

APPENDIX A –CHEMICAL TRANSFORMATION MECHANISMS

MGLY => C2O3 + HO2 + CO	PHOT	21	1				
O + ISOP => 0.750*ISPD + 0.500*FORM + 0.250*XO2 + 0.250*HO2 + 0.250*CXO3 + 0.250*PAR	CONS	3.60E-11					
OH + ISOP => 0.912*ISPD + 0.629*FORM + 0.991*XO2 + 0.912*HO2 + 0.088*XO2N	ARRH	2.54E-11	-407.6				
O3 + ISOP => 0.650*ISPD + 0.600*FORM + 0.200*XO2 + 0.066*HO2 + 0.266*OH + 0.200*CXO3 + 0.150*ALDX + 0.350*PAR + 0.066*CO	ARRH	7.86E-15	1912				
NO3 + ISOP => 0.200*ISPD + 0.800*NTR + XO2 + 0.800*HO2 + 0.200*NO2 + 0.800*ALDX + 2.400*PAR	ARRH	3.03E-12	448				
OH + ISPD => 1.565*PAR + 0.167*FORM + 0.713*XO2 + 0.503*HO2 + 0.334*CO + 0.168*MGLY + 0.252*ALD2 + 0.210*C2O3 + 0.250*CXO3 + 0.120*ALDX	CONS	3.36E-11					
O3 + ISPD => 0.114*C2O3 + 0.150*FORM + 0.850*MGLY + 0.154*HO2 + 0.268*OH + 0.064*XO2 + 0.020*ALD2 + 0.360*PAR + 0.225*CO	CONS	7.10E-18					
NO3 + ISPD => 0.357*ALDX + 0.282*FORM + 1.282*PAR + 0.925*HO2 + 0.643*CO + 0.850*NTR + 0.075*CXO3 + 0.075*XO2 + 0.150*HNO3	CONS	1.00E-15					
ISPD => 0.333*CO + 0.067*ALD2 + 0.900*FORM + 0.832*PAR + 1.033*HO2 + 0.700*XO2 + 0.967*C2O3	PHOT	22	0.0034				
TERP + O => 0.150*ALDX + 5.12*PAR	CONS	3.60E-11					
TERP + OH => 0.750*HO2 + 1.250*XO2 + 0.250*XO2N + 0.280*FORM + 1.66*PAR + 0.470*ALDX	ARRH	1.50E-11	-449				
TERP + O3 => 0.570*OH + 0.070*HO2 + 0.760*XO2 + 0.180*XO2N + 0.240*FORM + 0.001*CO + 7.000*PAR + 0.210*ALDX + 0.390*CXO3	ARRH	1.20E-15	821				
TERP + NO3 => 0.470*NO2 + 0.280*HO2 + 1.030*XO2 + 0.250*XO2N + 0.470*ALDX + 0.530*NTR	ARRH	3.70E-12	-175				
SO2 + OH => SO3 + HO2	TROE	3.00E-31	-3.3	1.50E-12	0	0.6	
OH + ETOH => HO2 + 0.900*ALD2 + 0.050*ALDX + 0.100*FORM + 0.100*XO2	ARRH	6.90E-12	230				

APPENDIX A –CHEMICAL TRANSFORMATION MECHANISMS

OH + ETHA => 0.991*ALD2 + 0.991*XO2 + 0.009*XO2N + HO2	ARRH	8.70E-12	1070					
NO2 + ISOP => 0.200*ISPD + 0.800*NTR + XO2 + 0.800*HO2 + 0.200*NO + 0.800*ALDX + 2.400*PAR	CONS	1.50E-19						
OLE + OH => OLE + OH + 0.0001*CG1 + 0.0149*CG2	CONS	3.20E-11						
PAR + OH => PAR + OH + 0.0018*CG3	CONS	8.10E-13						
XYL + OH => XYL + OH + 0.023*CG4 + 0.046*CG5	ARRH	2.00E-11	-116					
TOL + OH => TOL + OH + 0.033*CG6 + 0.083*CG7	ARRH	1.80E-12	-355					
TERP + OH => TERP + OH + 0.028*CG8 + 0.061*CG9	ARRH	1.50E-11	-449					
TERP + O3 => TERP + O3 + 0.089*CG10 + 0.033*CG11	ARRH	1.20E-15	821					
ISOP + OH => ISOP + OH + 0.232*CG12 + 0.0288*CG13	ARRH	2.54E-11	-407.6					
OLE + OH => OLE + OH + 0.0001*CG1 + 0.0149*CG2	CONS	3.20E-11						
PAR + OH => PAR + OH + 0.0018*CG3	CONS	8.10E-13						



The Centre for Australian Weather and Climate Research is a partnership between CSIRO and the Bureau of Meteorology.